Effect of Profilin on Actin Critical Concentration: A Theoretical Analysis

Elena G. Yarmola,*† Dmitri A. Dranishnikov,*† and Michael R. Bubb*†
*North Florida/South Georgia Veterans Health System, Research Service, Gainesville, Florida; and †University of Florida, Department of Medicine, Gainesville, Florida

ABSTRACT To explain the effect of profilin on actin critical concentration in a manner consistent with thermodynamic constraints and available experimental data, we built a thermodynamically rigorous model of actin steady-state dynamics in the presence of profilin. We analyzed previously published mechanisms theoretically and experimentally and, based on our analysis, suggest a new explanation for the effect of profilin. It is based on a general principle of indirect energy coupling. The fluctuation-based process of exchange diffusion indirectly couples the energy of ATP hydrolysis to actin polymerization. Profilin modulates this coupling, producing two basic effects. The first is based on the acceleration of exchange diffusion by profilin, which indicates, paradoxically, that a faster rate of actin depolymerization promotes net polymerization. The second is an affinity-based mechanism similar to the one suggested in 1993 by Pantaloni and Carlier although based on indirect rather than direct energy coupling. In the model by Pantaloni and Carlier, transformation of chemical energy of ATP hydrolysis into polymerization energy is regulated by direct association of each step in the hydrolysis reaction with a corresponding step in polymerization. Thus, hydrolysis becomes a time-limiting step in actin polymerization. In contrast, indirect coupling allows ATP hydrolysis to lag behind actin polymerization, consistent with experimental results.

INTRODUCTION

Profilin is one of the most important proteins in the regulation of actin polymerization. It was first discovered as a factor that causes actin depolymerization in vitro (1), yet is now almost exclusively described as a promoter of actin polymerization. The molecular mechanism of the profilin function is still unknown. Recent studies suggest that profilin accelerates both polymerization and depolymerization at the barbed end of actin filaments (2–5). Profilin forms a 1:1 complex with monomeric actin and sequesters it from pointed-end polymerization, catalyzes exchange of the actin-bound nucleotide, inhibits actin filament nucleation, localizes actin monomers by interactions with other actin-binding proteins such as formin and vasodilator-stimulated phosphoprotein, and decreases actin critical concentration (2,6–12). Actin critical concentration, A_c, is a very important value that indicates whether actin filaments would polymerize or depolymerize at particular conditions. At steady state, it is equal to the concentration of free globular actin, which is not in complex with other proteins. A_c provides a scale for total sequestered, unpolymerized actin at steady state (see our recent review (5) for details). As we discuss in Yarmola and Bubb (5), the observation that a complex of profilin and actin could add to the barbed ends of growing filaments (6) is sometimes misleadingly considered an explanation for the effect of profilin on A_c. It is important to note that this observation by itself cannot explain the effect of profilin on critical concentration (5,9). Although copolymerization would lower A_c, profilin-actin does not form a true copolymer with actin, as strong evidence shows that profilin must dissociate from the filament end before the next actin subunit or profilin-actin complex can add. Some models allow the addition of two profilin molecules (one for each strand) to the barbed end (13), but this hypothesis does not change the general idea and conclusions.

An idea that the effect of profilin on A_c may be explained by the coupling of the energy of ATP hydrolysis by filamentous actin to the profilin-related pathway in actin polymerization was first suggested by Pantaloni and Carlier in 1993 (7). This idea involves the concept of a thermodynamic energy square. The thermodynamic energy square describes the interdependence of the equilibrium and/or rate constants for two different pathways in actin filament elongation in the presence of profilin (2,4,5,7,9). As illustrated by Fig. 1, because either G-actin or the profilin-actin complex can bind to a barbed filament end, there are two possible pathways for actin filament elongation in the presence of profilin: a direct pathway g shown with a gray arrow and a profilin-related pathway pg shown with three purple arrows. In the absence of profilin, there is only one direct pathway. The energy difference between the two pathways in actin polymerization is $\Delta G'^{0}_{pg} - \Delta G'^{0}_{g} = -RT \ln \Phi$, where Φ is a ratio of the rate and equilibrium constants for the two elongation pathways (see Fig. 1). It is important to note that only an ''apparent'' energy square for actin polymerization involving ATP hydrolysis that relates apparent constants and does not distinguish between different nucleotide identities of actin subunits is allowed to be misbalanced.

Since for each pure form there is no ATP hydrolysis and therefore no interconversion between forms involved, there is no energy input in the case of pure form. We use the term ''pure form'' to refer to a hypothetical polymerization reac-

Submitted April 10, 2008, and accepted for publication August 22, 2008.

Address reprint requests to Elena G. Yarmola, University of Florida, Dept. of Medicine, PO Box 100221, Gainesville, FL 32610. Tel.: 352-376-1611 ext. 4305; Fax: 352-271-4547; E-mail: yarmola@ufl.edu.

Editor: E. Michael Ostap.

0006-3495/08/12/5544/30 $2.00

doi: 10.1529/biophysj.108.134569

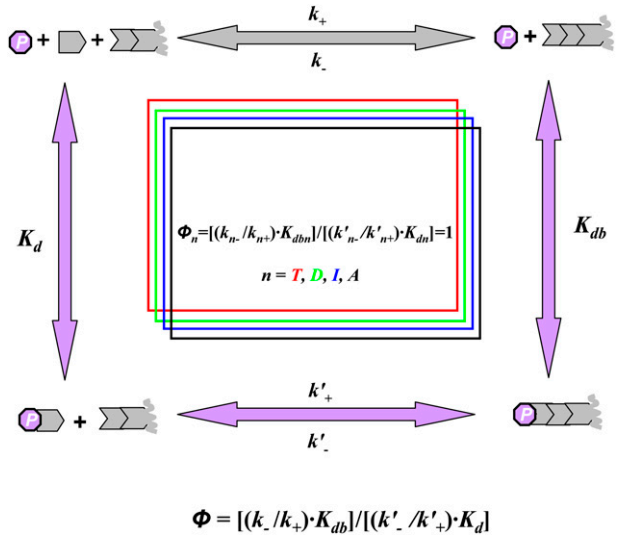

FIGURE 1 Two pathways of actin filament elongation in the presence of profilin and the thermodynamic energy square. G-actin is shown as a gray pentagon. Profilin is shown as a purple octagon. F-actin subunits are represented by a chevron, and filaments are depicted as one or more chevrons with a filament end opposite to the open side of a chevron. In the presence of profilin, there are two possible pathways for actin filament elongation. The gray arrow shows the direct pathway (*g*)—direct elongation through binding of G-actin subunits to the barbed end to obtain a filament one subunit longer. Three purple arrows show the profilin-related pathway (*pg*) through the binding of profilin to G-actin, formation of profilin-actin complex, then binding of the profilin-actin complex to the barbed end with subsequent dissociation of profilin. Only an ''apparent'' energy square that relates apparent constants and does not distinguish between different nucleotide identities of actin subunits is allowed to be misbalanced, and therefore only the apparent parameter Φ may not be equal to one. Each energy square that is limited to a particular form of subunit *n* must necessarily be balanced with $\Phi_n = 1$. The subscript *n* denotes the four actin subunit forms: ATP-, ADP-, ADP-Pi-bound, and nucleotide-free. The particular energy squares are shown as four colored squares.

tion involving actin subunits with identical nucleotide composition (either ATP- ADP-, or ADP-carrying subunits with bound phosphate (ADP-Pi), or nucleotide-free subunits). Detailed balance equations or balanced energy squares are applicable for pure forms so that each energy square that is limited to a particular form of subunit *n* must necessarily have $\Phi_n = 1$ (Fig. 1). The apparent ratio Φ, when not distinguishing between actin nucleotide forms which undergo conversion to each other in the presence of ATP, can deviate from 1. According to experimental data from different groups, Φ varies between 1 and 14 for muscle actin (7,14) and is as high as 33 for nonmuscle actin (2). As we discuss below in the ''Results'' and ''Discussion'' sections, the apparent parameter Φ depends, in general, on profilin concentration. This dependence may in part explain different results obtained by different groups.

Several possible mechanisms for the effect of profilin on A_c have been previously suggested:

I. Change of the contribution of the barbed end relative to that of the pointed end to actin dynamics. This mechanism suggested by us in Yarmola and Bubb (4) is based on the difference between critical concentrations A_{cb} and A_{cp} for the two-actin filament ends, barbed and pointed, correspondingly, and on the selective binding of profilin-actin complex to the barbed end. This selective binding changes the relative contribution of polymerization and depolymerization events occurring on the two ends, shifting critical concentration from the value intermediate between the specific critical concentrations for the pointed and barbed ends toward the lower barbed-end critical concentration (4,5).

II. Acceleration of ADP-ATP exchange by G-actin. This mechanism was suggested by Perelroizen et al. (15). Because actin filaments hydrolyze bound ATP and ADP-actin has a higher critical concentration than ATP-actin, ATP hydrolysis by actin filaments could lead to accumulation of monomeric ADP-bound actin at steady state and thus to higher A_c (15,16) if exchange of bound ADP for ATP by monomeric actin is not fast enough. Because profilin accelerates nucleotide exchange (11), a shift in the ratio of ADP- to ATP-bound actin monomer caused by profilin might lead to a decrease in A_c.

III. Destabilization of ATP and ADP binding to nucleotide-free G-actin induced by profilin. This hypothesis was suggested by Kinosian et al. (2). It suggests that ATP hydrolysis is not necessary for the imbalance of the energy square and that the effect of profilin on A_{cb} could be explained by profilin-induced destabilization of ATP and ADP binding by G-actin. This destabilization is postulated to affect the apparent energy square for actin polymerization in the presence of an excess of either ATP or ADP.

IV. A mechanism based on the difference in affinity of profilin to ATP- and ADP-Pi-bound barbed ends. This hypothesis is widely accepted. It was first suggested by Pantaloni and Carlier (7) and further developed in subsequent works (15,17–19). A variation of this mechanism has also been developed by others (20,21). It assumes direct incorporation of ATP hydrolysis energy into the profilin-related pathway *pg* (Fig. 1) and apparent energy square misbalance. According to this mechanism, profilin-actin complex (PA) binds to the barbed end of an actin filament and remains bound until the end actin subunit hydrolyzes ATP. Upon hydrolysis, profilin (P) dissociates from the end of actin filaments since the affinity of profilin to the ADP-Pi-bound end is lower than it is to the ATP-bound one. After profilin dissociation, the actin filament is one subunit longer, and profilin can bind another G-actin subunit and deliver it to the barbed end, as in the previous cycle. In this model ATP hydrolysis is a rate-limiting step in barbed-end polymerization in the presence of profilin (17). Therefore, acceleration of ATP hydrolysis by profilin has been suggested (17,19) so that polymerization rates can correspond to in vivo observations.

V. A mechanism based on the acceleration of the process of exchange diffusion by profilin. This mechanism was

suggested by us in Yarmola and Bubb (5). It assumes that ATP hydrolysis events may occur independent of profilin dissociation and that energy coupling occurs indirectly through the fluctuation-based process of exchange diffusion. At conditions of excess ATP, exchange diffusion enriches filament ends with ATP-carrying subunits, thus increasing the number of subunits on the filament tip that can simultaneously undergo ATP hydrolysis. Profilin may accelerate exchange diffusion, thereby increasing the average rate of ATP hydrolysis per filament, although such hydrolysis is not rate limiting for actin polymerization.

There are several important processes occurring in actin polymerization dynamics in the presence or absence of profilin: nucleotide exchange by monomeric actin, ATP hydrolysis, and inorganic phosphate release by polymeric actin, treadmilling, and exchange diffusion (Fig. 2). The term ''treadmilling'' was first introduced by Wegner (22). In treadmilling, there is continuous net dissociation of ADP-carrying subunits from the pointed end. These dissociated monomeric subunits exchange bound ADP for ATP (nucleotide exchange) and then they or other ATP-carrying subunits bind to the opposite, barbed end, move along the filament, and undergo hydrolysis on their way. The process of exchange diffusion was first studied in 1983 by Brenner and Korn (23). It is a process similar to treadmilling, but dissociation and binding occur at the same end (barbed or pointed) rather than opposite ends. Both treadmilling and exchange diffusion include nucleotide exchange by monomeric actin and inorganic phosphate release by polymeric and monomeric actin (Fig. 2).

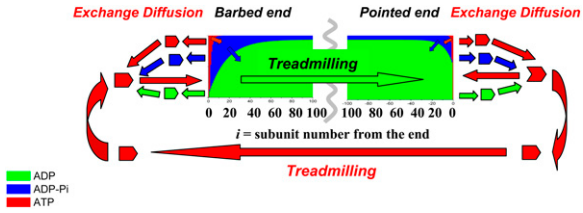

FIGURE 2 Illustration of the terms ''treadmilling'' and ''exchange diffusion''. Actin filaments are represented by an average filament nucleotide profile where ATP-bound actin is shown in red, ADP- and inorganic phosphate (Pi) bound is shown in blue, ADP-bound actin is shown in green, and nucleotide-free actin is not shown. *i* is the distance from the filament end in number of subunits. The relative height of a color at any *i* reflects the percentage of that subunit at that *i*. The monomeric subunits are shown as pentagons of the corresponding color. Short arrows show the association and dissociation of the actin subunits from the filament ends, exchange of the bound nucleotide by G-actin subunits, and hydrolysis of bound ATP or inorganic phosphate release by F-actin subunits. Long arrows are related to the process of treadmilling. In treadmilling, the ADP-carrying subunits dissociate from the pointed end, exchange bound ADP for ATP, and then bind to the opposite, barbed end, move along the filament, and undergo hydrolysis on their way. Exchange diffusion is a similar process, but dissociation and binding occur at the same end (barbed or pointed) rather than opposite ends, such that the hydrolyzed actin subunits (ADP or ADP-Pi bound) dissociate from the end, exchange ADP (or ADP-Pi) for ATP, and then bind to the same end.

In 2004, Bindschadler et al. (24) built a mechanistic model of actin steady-state dynamics that predicted the full nucleotide composition of steady-state filaments for the first time. Their model provides useful insights into actin polymerization in the presence of ATP. However Bindschadler et al. assumed that ''profilin-actin deposits ATP-bound subunits at barbed ends and then [profilin] instantly decouples from filaments''. This assumption is equivalent to the assumption of very large or infinite energy input coupled to the profilin pathway (4,5,7). As mentioned above, it is not valid for any pure form and instead detailed balance equations are applicable. The goal of this work was to create a model providing an explanation for the effect of profilin on A_c consistent with thermodynamic constraints and experimental results.

Our model is based on the same approach utilized by Bindschadler et al. (24): we considered polymerization of four different actin forms (ATP- or ADP-carrying, ADP-carrying subunits with bound phosphate (ADP-Pi), and nucleotide-free subunits) at steady state in the presence and absence of profilin, although we utilize strong thermodynamic constraints. Four thermodynamic energy squares, each limited to a pure form of subunits (including ATP-bound subunits), are each thermodynamically balanced because the permissible reactions between profilin and actin involve no energy input from ATP hydrolysis (see Fig. 1). With this model, we were able to theoretically evaluate possibilities III–V for the effect of profilin on the barbed-end critical concentration A_{cb}. In addition, we evaluate mechanism II experimentally.

In this work, we do not evaluate mechanism I. This mechanism does not directly require energy imbalance, which may come from ATP hydrolysis by filamentous actin. Neither does it exclude the possibility of energy imbalance, so the other mechanisms may be simultaneously active. Although this mechanism does not require energy imbalance, it does require ATP hydrolysis, without which there is no difference between the barbed and pointed ends' critical concentrations (22). In addition, this is the only mechanism considered requiring a difference between the two ends of an actin filament and hence the only mechanism that may involve actin filament treadmilling. The last four mechanisms (II–V) do not require the existence of the second filament end and, therefore, do not involve or require treadmilling, but are based on the interconversion of the four different nucleotide forms of actin subunits, each of which have different polymerization properties.

Since mechanism I is the only one that requires two filament ends, limitation of the modeling to one-end dynamics eliminates mechanism I and allows evaluation of other possibilities. Similarly, it might be assumed that experimental elimination of dynamics at the pointed end would allow the determination of the contribution, if any, of mechanisms other than mechanism I. Unfortunately, we have evidence that it is difficult to unambiguously eliminate all actin subunit reactions at the pointed end using previously identified ''capping proteins'' or similar methods. In summary, we know

mechanism I has been previously shown to contribute to the determination of A_c, whether theoretical or actual, but the other mechanisms have little or no previously reported experimental support and are thus theoretical in nature. The purpose of this work is to perform a theoretical analysis of the contributions of each potential mechanism by which profilin affects A_c that can be used in future investigations to design and implement experimental tests of each mechanism.

EXPERIMENTAL PROCEDURE

Materials

Rabbit skeletal muscle Ca^{2+}-actin was prepared from frozen muscle (Pel-Freez, Rogers, AR) in buffer G (5.0 mM Tris-HCl, 0.2 mM ATP, 0.2 mM dithiothreitol, 0.1 mM CaCl2, and 0.01% sodium azide, pH 7.8), and pyrenyl-labeled actin (actin labeled on Cys-374 with *N*-(1-pyrene) iodoacetamide) was prepared with 0.7–0.95 mol of label/mol of protein using the method of Kouyama and Mihashi (25). Recombinant human thymosin β_4 and profilin I were purified as previously described (26,27). The thymosin β_4 contained an added C-terminal cysteine. The cysteine-modified thymosin β_4 was labeled as previously described (26,27) with tetramethylrhodamine 5-maleimide. Previous results confirm that the labeled, C-terminal cysteine-modified thymosin β_4 has identical actin binding properties as wild-type thymosin β_4 (26,27).

Steady-state experiment

One percent pyrene-labeled Mg^{2+} F-actin (10 μM) was diluted immediately upon reaching saturation level of polymerization to indicated final concentrations in the same polymerization buffer (5 mM Tris-HCl, pH 7.9, 0.1 mM $CaCl_2$, 0.125 mM EGTA, 2 mM $MgCl_2$, 40 mM KCl; the predicted free Ca^{2+} concentration for this buffer is 44.5 nM) in the absence or presence of indicated amounts of profilin. Samples were incubated at room temperature for 24 h, and then pyrene fluorescence and fluorescence anisotropy measurements were done (both for the same samples) as described below.

The pyrene fluorescence assay

The pyrene fluorescence assay is based on the observation that fluorescence of actin labeled on Cys-374 with *N*-(1-pyrene) iodoacetamide is ~20 times higher when actin is in polymerized (F-) state compared to that for unpolymerized (globular, or G-) state. Thus when total actin concentration is known, this method provides concentrations of F-actin and the concentration of total G-actin (the sum of all nucleotide forms and all complexes with G-actin binding proteins) (7,25).

The fluorescence anisotropy critical concentration assay

The fluorescence anisotropy critical concentration assay is based on the fact demonstrated by us in Yarmola and Bubb (4) that thymosin β_4 does not bind to filamentous actin with any significant affinity, although it binds with relatively high affinity to monomeric actin. Others and we have made frequent use of steady-state fluorescence anisotropy measurements to determine the equilibrium binding of various fluorescently labeled actin-binding proteins to actin (26–28). The binding isotherm for thymosin β_4-G-actin interaction, when plotted as anisotropy versus total actin for trace levels of rhodamine-labeled thymosin β_4, provides a standard curve for determination of the free G-actin concentration in any sample in which the anisotropy is determined under the same standard conditions (see Yarmola and Bubb (4) for details). Only trace amounts of labeled peptide (10–100 nM) are required. Since the affinity of thymosin β_4 to ATP-bound G-actin is ~20 times higher than of that for the ADP-bound G-actin, the fluorescence anisotropy assay is much more sensitive to the ATP actin form than to the ADP form.

The fluorescence anisotropy data collection

Data were collected on a Photon Technology International (South Brunswick, NJ) spectrofluorometer. Tetramethylrhodamine-5-maleimide-labeled thymosin β_4 was excited with vertically polarized light at 546 nm. The horizontal (I_h) and vertical (I_v) components of the emitted light are detected at 575 nm for 0.3-ml samples in glass cuvettes. The fluorescence anisotropy, r, is calculated using $r = (I_v - G \times I_h)/(I_v + 2G \times I_h)$. The G-factor is determined for the peptide in solution excited with horizontally polarized light and averaged over all measurements. Bound actin does not change the total fluorescence intensity of the rhodamine-labeled thymosin β_4 (28), so the observed anisotropy r is a linear function of the fraction of thymosin β_4 that is bound to actin: $r = (r_b \times [T_b] + r_f \times [T_f])/[T_0]$, where r_f is anisotropy of free thymosin T_f, r_b is anisotropy of thymosin bound to actin T_b, and $[T_0] = [T_f] + [T_b]$ where the $[T_f]$ and $[T_b]$ are concentrations of T_f and T_b, correspondingly. Any sample containing an unknown concentration of free actin (A_c, if at steady state) is assayed using conditions identical to those of the standards (see Yarmola and Bubb (4) for details).

MATHEMATICAL MODEL

Reactions and variables

Variables are defined in Table 1. Chemical reactions, parameter definitions, and thermodynamic constraints are shown in Fig. 3. Part 1 of Appendix 1 provides equations for the chemical reactions shown in Fig. 3. The only irreversible reaction is the hydrolysis of ATP by ATP-bound F-actin subunits. All other reactions are reversible: i), the binding of ATP and ADP to the nucleotide-free G-actin form and its complex with profilin, ii), the binding of inorganic phosphate (Pi) to ADP-bound G- and F-actin subunits and their complexes (when applicable) with profilin, iii), the binding of each nucleotide form of G-actin and their complexes with profilin to the filament ends, and iv), the binding of profilin to monomeric actin subunits and to the filament ends of each nucleotide type.

Assumptions, idealizations, and constraints

1. The model considers polymerization of four actin subunit forms: ATP-, ADP-, ADP-Pi-bound, and nucleotide-free. The elongation and depolymerization rate constants for each form depend only on the nucleotide type of associating or dissociating monomers. The elongation rate does not depend on the nucleotide state of the filament tip subunits, and the rate of dissociation does not depend on the nucleotide state of any filamentous subunits except the one dissociating from the filament tip. The same applies to the complexes of each form with profilin. Profilin (or profilin-actin complex) has to dissociate from the filament end before the next actin subunit or profilin-actin complex can bind.
2. Hydrolysis of ATP within filaments occurs randomly and irreversibly. For all actin filament subunits except the terminal ones, the rates of hydrolysis and phosphate release and binding depend neither on the position of the subunit in the filament nor on the identity of the neighboring subunits. For the terminal subunits, the rates of ATP hydrolysis and phosphate binding and release may differ from the corresponding rates for the interior subunits, although the phos-

TABLE 1 Definition of Variables

Variable	Description
T	Concentration of ATP-bound free G-actin (ATP-bound monomeric actin that is not in complex with any of the actin-binding proteins)
D	Concentration of ADP-bound free G-actin
I	Concentration of ADP-Pi-bound free G-actin
A	Concentration of nucleotide-free free G-actin
n	T, D, I, or A. All summations $\sum$ by n are for $n = T, D, I, A$
A_c	Critical concentration: total concentration of free monomeric actin—sum of all nucleotide forms: $A_c = \sum n$
r_n	Fraction of the particular nucleotide form in the total free monomeric actin pool: $r_n = n/A_c$; $\sum r_n = 1$
P	Concentration of free profilin (not in complex with actin)
$[Pn]$	Concentration of profilin in complex with actin monomer of a certain nucleotide type
[ATP]	Concentration of ATP
[ADP]	Concentration of ADP
[Pi]	Concentration of inorganic phosphate
i	Distance from the filament end. The distance is measured in terms of i, the number of subunits so that $i = 0$ always corresponds to G-actin and $i = 1$ always corresponds to the end subunit. i is a natural number from 1 to ∞. All $\sum$ by i are for i from 1 to ∞.
$g_{n(i)}$	Fraction of subunits at position i in the filament that are bound to a certain nucleotide type and not bound to profilin (or an average probability for the subunit at position i to carry a certain type of nucleotide and not to be bound to profilin)
g_f	Fraction of filament ends free (not bound to profilin): $g_f = \sum g_{n(1)}$
g_n	Fraction of the uncapped filament ends bound to a certain nucleotide type: $g_n = g_{n(1)}/g_f$
$g_{Pn(1)}$	Fraction of subunits at position $i = 1$ (filament end) that are bound to a certain nucleotide type and to profilin
g_P	Fraction of filament ends bound to profilin (capped): $g_P = \sum g_{Pn(1)}$; $g_f + g_P = 1$
K_{db}	Apparent equilibrium dissociation constant for the addition of profilin to F-actin on the barbed end (defined experimentally): $g_f = (1 + P/K_{db})^{-1}$
k_{0+}	Apparent rate constant for the addition of actin monomers to the filament end in the presence of the excess ATP and absence of profilin
k_{0-}	Apparent rate constant for the dissociation of actin monomers from the filament end in the presence of the excess ATP and absence of profilin
A_{cb}	Barbed-end critical concentration in the presence of ATP
A_{cp}	Pointed-end critical concentration in the presence of ATP
k_{ON}	Net rate of polymerization
k_{OFF}	Net rate of depolymerization
E	Steady-state flux of subunit exchange: $E = k_{ON} = k_{OFF}$

phate affinity to the end subunit is the same as the affinity for the interior subunits.

3. Profilin binding and dissociation from G-actin and filament ends is assumed fast enough that at any moment, the concentration of the complex of profilin with each G-actin form and the percentages of the uncapped ends of each type are defined by the corresponding equilibrium dissociation constants.
4. There are four balanced thermodynamic energy squares, each limited to a specific nucleotide form of actin subunit. This and other thermodynamic constraints are shown in Fig. 3 in boxes.
5. The modeling is limited to the consideration of one-end dynamics only. The filaments are assumed to be long enough to contain a core of ADP- and ADP-Pi-carrying subunits in which the content of the ADP-Pi-carrying subunits is defined by the phosphate affinity to the filamentous ADP-bound subunits. The assumption of the existence of an ADP and ADP-Pi core and the way we have numbered subunits in the filament allow us to remove all limitations on the filament length distribution (although this distribution is not calculated here). Note that A_c depends neither on the core length distribution nor on the core length itself. Only the lengths of ATP and ADP-Pi caps are important, and their length distributions are established by polymerization-depolymerization dynamics. In our model, i is the distance from the filament end, and $i = 1$ is always assigned to the end subunit (see Fig. 3 and Table 1 for variable and parameter definitions). Since the value of i is not limited, the highest values of i correspond to the ADP and ADP-Pi core. Thus, the effect of the ATP and ADP-Pi caps is automatically taken into consideration. For the filament nucleotide profile, we will calculate average probabilities $g_{n(i)}$ for subunits at position i to be bound to a certain nucleotide type and an average length of the filament's ATP cap, which in the case of random hydrolysis is equal to the sum of probabilities for all subunits in the filament to carry ATP. The results obtained from the model are applicable (separately) for both barbed and pointed ends with corresponding parameters.
6. The system is at steady state.

Applicability and potential limitations

Assumptions 5 and 6 have been tested both in theory and by experiment for a limited set of experimental conditions. For pointed-end dynamics, these assumptions correspond to the steady-state conditions in a test tube when the barbed ends are capped and the filaments are long enough to have the ADP-ADP-Pi core. Our results predict that to satisfy this assumption for the pointed end, filaments need to be longer than ~50 subunits. For the barbed end in the absence of

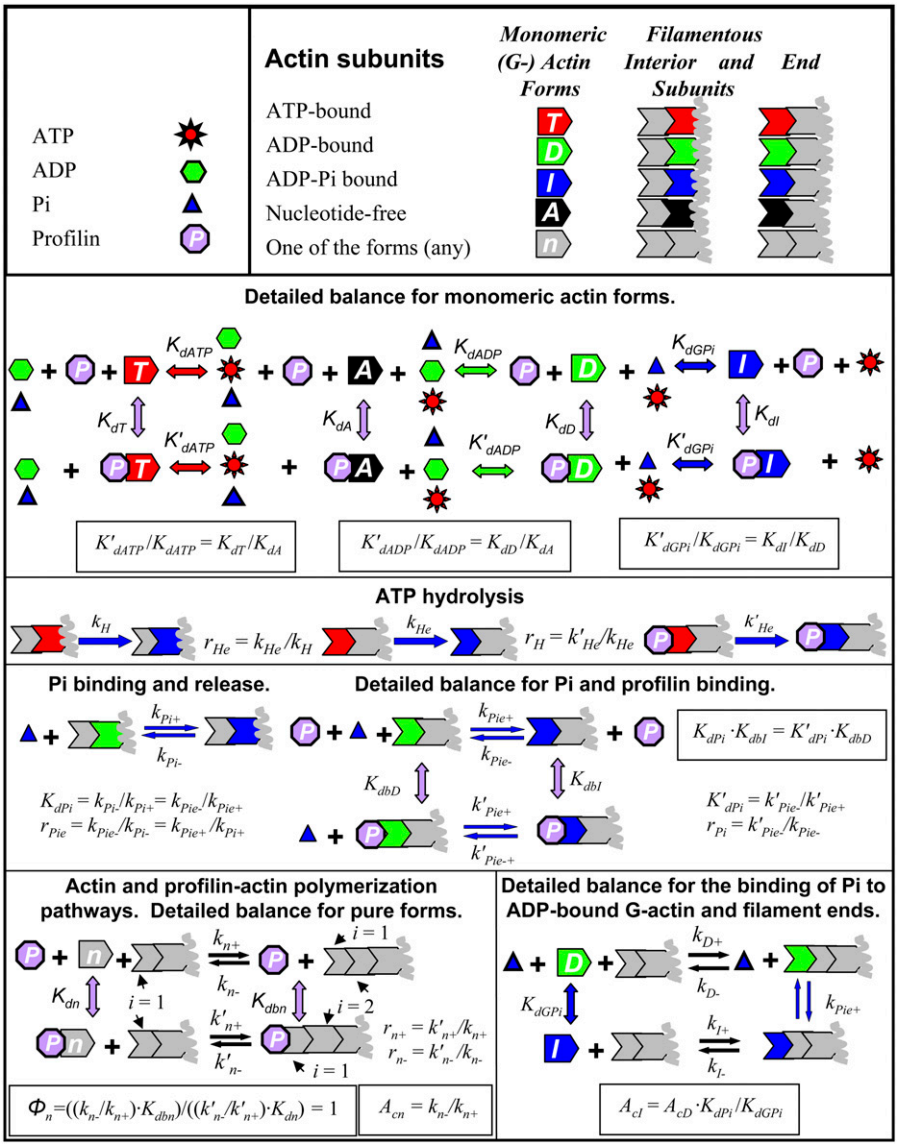

FIGURE 3 Chemical reactions considered in the model with parameter definitions and thermodynamic constraints. The model considers a steady-state copolymerization of four monomeric actin forms: ATP- (*T*), ADP- (*D*), ADP- and Pi-bound (*I*), and nucleotide-free (*A*). *T* is shown in red, *D* in green, *I* in blue, and *A* in black. Actin subunits that could have any type of bound nucleotide are shown in gray. Monomeric and filamentous subunits are shown as in Fig. 1 with the color corresponding to bound nucleotide. The distance from the filament end is measured in terms of *i*, the number of subunits, so that $i = 0$ corresponds to G-actin, and $i = 1$ always corresponds to the subunit at the filament end. ATP hydrolysis by ATP-bound filamentous actin subunits is the only irreversible reaction. All other reactions are reversible: i), Binding of ATP (*red sun*) or ADP (*green hexagon*) to *A* (or *PA*) to form *T* or *D* (or *PT* or *PD*). ii), Binding of inorganic phosphate Pi (*blue triangle*) to *D* (or *PD*), or the ADP-bound F-actin subunits (or the profilin-capped *D*-type filament ends) to form *I* (or *PI*), or the ADP-Pi bound F-actin form (or the profilin-capped *I*-type filament ends). iii), Each nucleotide form of G-actin and their complexes with profilin bind to the filament ends. iv), Profilin (*purple octagon*) binds to monomeric actin subunits and to the filament ends of each nucleotide type. Thermodynamic constraints are shown in boxes. Parameter definitions are shown next to reactions (without *boxes*).

profilin, the filaments must be at least 80–100 subunits long, and in the presence of profilin, at least 300 subunits long (see filament nucleotide profiles on Fig. 9). As reported by Sept et al. (29), steady-state length distributions for uncapped actin filaments in the absence of profilin are exponential with a mean of ~7 μm (2600 subunits). An average length of 22.3 and 19.7 μm (8300 and 7300 subunits) is reported by Kovar et al. (30) in the absence and presence of profilin, correspondingly. With exponential distribution and the average length of 7 μm, 96% of filaments should be longer than 100 subunits, and 89% are longer than 300 subunits, and with the average length of 20 μm, 98.7% of all filaments should be longer than 100 subunits, and 96% are longer than 300 subunits. Thus, most filaments should have the ADP-ADP-Pi core at these conditions.

Again note that the rationale for considering dynamics at each end separately is to eliminate the contribution of mechanism I, and therefore to permit the analysis (and ultimately experimental determination) of the contribution of other potential mechanisms that explain how profilin modulates A_c. Ultimately, both ends must be considered simultaneously, but the only potential influence they have on one another is by generating differences in A_c. In fact, mechanism I rigorously accounts for how profilin modulates A_c in the presence of multiple filament ends with different end-specific critical concentrations. Thus, limiting the model to one-end dynamics will, in general, have an impact on the resulting A_c since mechanism I (requiring the presence of the second filament end) is excluded from consideration. In contrast, experimental conditions with both barbed and pointed ends present will be influenced by mechanism I. Applicability of the one-end dynamics model to in vivo conditions is discussed in the section ''Implications for possible in vivo effects of profilin''.

RESULTS

Solution for A_c and filament nucleotide profile

The actin critical concentration A_c is defined by

$$A_c^{-1} = \sum r_n \times U_n^{-1} \times A_{cn}^{-1}, \quad (1)$$

where $A_{cn} = k_{n-}/k_{n+}$ are critical concentrations for pure actin forms which do not depend on profilin concentration. As defined in Table 1, r_n are fractions of particular nucleotide forms in total monomeric actin. Coefficients U_n are correction factors for the rates of depolymerization of specific nucleotide forms and account for the conversion of the form n in filamentous actin to other forms that have different depolymerization rate constants. The physical meaning of the coefficients U_n is discussed in more detail in the section ''Actin steady-state dynamics in the presence of profilin''. Part 2 of Appendix 1 provides the derivation of the analytical equations for A_c, U_n, and the filament nucleotide profile $g_{n(i)}$ (see Eqs. A68–A72, A37–A40, and A50–A53 and Table 1 for definitions).

Note, that we do not provide a complete analytical solution for U_n, A_c, and the filament nucleotide profile $g_{n(i)}$ since coefficients C_A, C_T, and C_1 in Eqs. A57–A59 and variables E, α, and β in Eqs. A21, A63, and A64 are expressed through A_c and g_f. Instead, we solved this system numerically for the case when mechanism II is inactive (see discussion regarding mechanism II below). A computer program named ABAKUS, an acronym for Actin-Binding Activities and Kinetic solUtionS, available for any interested researcher (31) calculates A_{cb}, A_{cp}, and other values of interest as a function of the concentration of inorganic phosphate Pi, free profilin concentration P or any other parameter of the user's choice. Total profilin concentration can be obtained as the program output along with A_c and other values of interest. The program allows the adjustment of the rate and equilibrium constants and the ATP, ADP, and Pi concentrations. Default parameters correspond to those in Table 2, which summarizes kinetic and equilibrium constants obtained from the literature or derived from thermodynamic constraints. In addition, as shown subsequently, analysis of our resulting analytical equations allows useful insights into the mechanism of profilin action.

Actin steady-state dynamics in the absence of profilin

The roles of ATP hydrolysis and exchange diffusion in actin polymerization

In the absence of profilin, ATP hydrolysis on F-actin increases A_c if D- or I-type subunits dissociate from the filament tip faster than T-type subunits and decreases A_c otherwise. Throughout the text these possibilities are described as case A when $k_{Y-} \geq k_{T-}$ where index Y stands for either I or D, and case B when $k_{Y-} \leq k_{T-}$. They are described as ''cases'' because the applicability of case A or B depends on the concentration of inorganic phosphate as well as on the value of parameters not known with certainty. The effect of hydrolysis is reduced by exchange diffusion, which tends to bring the tip back to the T state.

The effects of hydrolysis and exchange diffusion follow from Eq. 1. Based on theoretical and experimental considerations discussed in the section concerning mechanism II,

TABLE 2 Parameters

k_H (s^{-1})	k_{Pi-} (s^{-1})	K_{dATP} (μM)	K_{dADP} (μM)	K_{dGPi} (mM)	K_{dPi} (mM)	[Pi] (μM)	[ATP] (μM)	[ADP] (μM)
0.3 (41)	0.0026 (39)	0.007 (39)	0.094 (39)	47*	1.5 (35)	100	1000	100
		Barbed	Barbed	Barbed	Barbed		Pointed	Pointed
		r_{He}	r_{Pie}	r_H	r_{Pi}		r_{He}	r_{Pie}
		1	8000 (35)	1	1		1	8000 (35)
		Barbed	Barbed	Barbed	Barbed		Pointed	Pointed
Form	K_{dn} (μM)	K_{dbn} (μM)	r_{n+}	k_{n-} (s^{-1})	k_{n+} ($s^{-1} \times \mu M^{-1}$)	A_{cn} (μM)	k_{n-} (s^{-1})	k_{n+} ($s^{-1} \times \mu M^{-1}$)
A	0.013 (39)	14.9†	0.8†	0.25†	7.4†	0.034‡	0.02¶	0.56†
						0.034§	0.007§	0.20†
T	0.099 (39)	14.9†	0.8 (2,17)	0.26‖	7.4 (32)	1.57¶	0.88‖	0.56 (32)
						0.035§	0.007‖§	0.20§
I	0.100†	14.9†	0.8†	0.20 (35)	3.4 (35)	0.059§	0.006§ (35)	0.11 (35)
D	0.120 (39)	14.9†	0.5 (2)	5.4 (35)	2.9 (35)	1.86§	0.26§‖ (35)	0.14 (35)
Barbed apparent	0.099 (39)	14.9 (2,4)	0.8 (2,17)	0.8 (32)	7.4 (32)	0.11¶ (32)		
Pointed apparent						0.79¶ (32), 0.79 (32)	0.44 (32) 0.16§	0.56 (32) 0.20§

*Obtained from the thermodynamic constraint $A_{cI} = A_{cD} \times K_{dPi}/K_{dGPi}$.
†Assumed to be similar to parameters for other forms.
‡Obtained from the thermodynamic constraint $A_{cAb} = A_{cAp} = A_{cA}$.
§All thermodynamic constraints (detailed balance) are satisfied for all forms.
¶Obtained from the thermodynamic constraints $A_c = k_{n-}/k_{n+}$.
‖Obtained from the analytical solution using experimental values for k_{0-} in the presence of ATP as derived in part 3 of Appendix 1 (Eq. A91).

the ATP-bound form is the predominant form of monomeric actin in excess ATP. Then Eq. 1 reduces to

$$A_c = A_{cT} \times U_T, \quad (2)$$

and the apparent rate of actin polymerization in the absence of profilin $k_{0+} \approx k_{T+}$ (index ''0'' stands for zero profilin). However, the apparent rate of depolymerization k_{0-} at these conditions is a weighted average of the depolymerization rate constants for all nucleotide forms:

$$k_{0-} = \sum g_{n(1)} \times k_{n-} = k_{T-} \times U_{T0} \neq k_{T-}, \quad (3)$$

where $g_{n(1)}$ are fractions of subunits at the filament tip that are bound to a certain nucleotide type (see Table 1). If ATP-bound subunits dissociate from the filament end slower than other forms (case A), hydrolysis is unfavorable for polymerization and leads to an increase in A_c compared to the value A_{cT} in the absence of hydrolysis. In case B, when ATP-bound subunits dissociate faster than other forms, hydrolysis may lead to the decrease in A_c and stabilization of polymer. As derived in part 1 of Appendix 2, in the limiting instance when ATP hydrolysis and phosphate release are immediate (or very fast compared to the polymerization-depolymerization dynamics), as was assumed by Wegner in (22),

$$k_{0-} = k_{D-} \quad \text{and} \quad A_c = k_{D-}/k_{T+}, \quad (4)$$

according to (22). In this instance,

$$U_T = k_{D-}/k_{T-}. \quad (5)$$

Since the hydrolysis and phosphate release are not immediate but have rates comparable to the rates of polymerization and depolymerization, exchange diffusion produces an effect opposite to that of ATP hydrolysis on both A_c and the nucleotide profile. Hydrolysis drives the nucleotide profile toward ADP-Pi- and ADP-actin, and exchange diffusion drives it toward ATP-actin. Thus, ATP hydrolysis and exchange diffusion effects are linked together in actin polymerization, and the resulting A_c depends on how effectively exchange diffusion eliminates the effect of ATP hydrolysis. The faster the subunit exchange compared to hydrolysis is, the closer A_c is to A_{cT}. Fig. 4 schematically illustrates mutual effects of ATP hydrolysis and exchange diffusion for two situations: when hydrolysis is slow compared to subunit exchange (*top panel*) and when hydrolysis is fast compared to exchange (*bottom panel*).

Difference between barbed- and pointed-end critical concentrations

Numerous experimental data suggest that in excess ATP and in the absence of profilin, experimentally measured critical concentrations for the barbed and pointed ends (A_{cb} and A_{cp}, correspondingly) are different (2–4,7,32,33, Table 2), which apparently contradicts the theory for equilibrium polymers (34). An explanation for the observed discrepancy is that actin polymerization in the presence of ATP involves ATP hydrolysis, and thus interconversion of forms, that creates a difference (22). As discussed above, at conditions with excess ATP, $k_{0+} \approx k_{T+}$ and k_{0-} is a weighted average of the depolymerization constants for different nucleotide forms. For experimental conditions, ATP hydrolysis cannot be prevented, and although nonhydrolysable ATP analogs are available for experimental study, they may both bind differently to actin than ATP and result in actin with different properties than ATP actin (2). Thus, parameters for the pure ATP form may only be estimated. In part 3 of Appendix 1, we derive an analytical solution for k_{T-} (and A_c) using the experimental values for k_{0-} in the presence of ATP and the absence of profilin (Eq. A91). This approach is useful since A_c in the absence of profilin is well established experimentally (2–4,7,32,33) and k_{T-}, as discussed above, is very difficult to obtain experimentally. The values of k_{T-} for the barbed and pointed ends in Table 2 were obtained using this solution (see section ''Effect of parameters on model predictions'' below).

Note, though, that for each pure form the constraint

$$A_{cnp} = A_{cnb} = A_{cn} \quad (6)$$

must be true. The index ''p'' refers to the pointed end, and the index ''b'' to the barbed end. Then one obtains from Eqs. 2 and 6

$$A_{cp}/A_{cb} = U_{Tp}/U_{Tb}, \quad (7)$$

and for the limiting case with immediate hydrolysis and phosphate release (see Eq. 5),

$$A_{cp}/A_{cb} = (k_{bT-}/k_{bD-})/(k_{pT-}/k_{pD-}). \quad (8)$$

Note that if the ratios of depolymerization rates are the same ($k_{bT-}/k_{bD-} = k_{pT-}/k_{pD-}$), there should be no difference between A_{cp} and A_{cb} in this case even if the rates of depolymerization (or polymerization) themselves are different.

As we mentioned above, since hydrolysis and phosphate release are not immediate, exchange diffusion produces an effect opposite to that of ATP hydrolysis. Since exchange diffusion on the barbed end is faster than exchange diffusion on the pointed end, it could more effectively eliminate the effect created by ATP hydrolysis, bringing A_c closer to A_{cT}. Thus, the difference in A_{cb} and A_{cp} is defined by a combination of two factors: 1), the difference in the depolymerization rates ratios (not the rates themselves), and 2), the difference in the rates of exchange diffusion. Treadmilling could also add to this process, affecting monomeric actin concentration and thus affecting the subunit exchange. Note that exchange diffusion is always present, whereas treadmilling can only occur when a difference between A_{cb} and A_{cp} already exists. Thus, treadmilling can only add to the other mechanisms.

Dependence of A_c on inorganic phosphate concentration

As demonstrated in part 2 of Appendix 2 for the limiting case (*i*), with moderate rates of depolymerization, slow phosphate release, and phosphate release unaffected by location on a

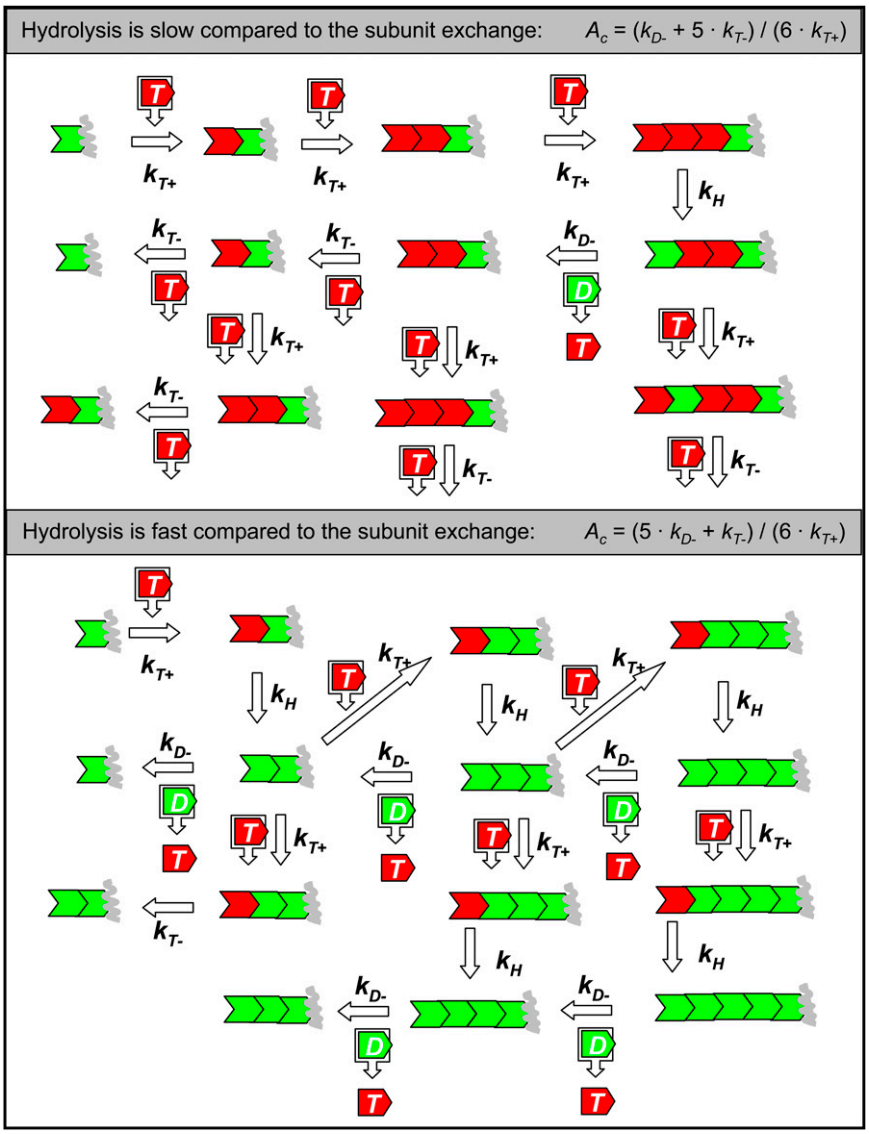

FIGURE 4 Schematic illustration of the effects of ATP hydrolysis and subunit exchange on the filament nucleotide profile and A_c. For simplicity, all globular actin is assumed to be predominately in the ATP-bound form (fast nucleotide exchange), Pi concentration is assumed to be very low, and Pi release is assumed to occur immediately after hydrolysis. Concentrations of the nucleotide-free (A) and ADP-Pi-bound (I) forms are therefore negligible; these forms are not shown. Only ATP- and ADP-bound actin forms are shown. Symbols are as in Figs. 1 and 3. The top panel illustrates the situation when hydrolysis is slow compared to the subunit exchange. In this situation, the event of hydrolysis is relatively rare compared to the association and dissociation events (one event of hydrolysis per six subunit association-dissociation events). Therefore the percentage of the ADP-bound subunits at the filament end is small, and depolymerization occurs predominantly through dissociation of the ATP-bound subunits with the corresponding apparent dissociation rate ($k_{0-} = (k_{D-} + 5 \times k_{T-})/6$). Therefore A_c is close to k_{T-}/k_{T+}. The bottom panel illustrates the situation when hydrolysis is fast compared to the subunit exchange. In this situation, hydrolysis occurs almost immediately after the association event (five events of hydrolysis before subunit dissociation per six subunit association-dissociation events), and therefore most of the ATP-bound subunits do not have a chance to dissociate before the ATP is hydrolyzed. They dissociate, therefore, as the ADP-bound subunits with corresponding rates ($k_{0-} = (5 \times k_{D-} + k_{T-})/6$). Thus depolymerization occurs predominantly through dissociation of the ADP-bound subunits, and A_c is close to k_{D-}/k_{T+}.

terminal subunit ($r_{Pie} \approx 1$, see Fig. 3 for parameter definitions), A_c depends mainly on parameters for ATP- and ADP-Pi actin forms and is not sensitive to the ADP-actin parameters and the concentration of phosphate. In contrast, as recently suggested by Fujiwara et al. (35), if phosphate dissociation from the terminal subunit is very much faster than in the interior with $r_{Pie} \gg k_H/k_{Pi-}$, the overall phosphate release will be much faster than hydrolysis. Then A_c is sensitive to only ATP- and ADP-actin parameters at low phosphate concentration and becomes sensitive to the ADP-Pi parameters only when the phosphate concentration increases. Our results and those previously reported by others support this alternative hypothesis and the resultant conclusion that $r_{Pie} \gg 1$. The observation that inorganic phosphate decreases the pointed and barbed-end critical concentrations in the presence of ATP, initially reported by Rickard and Sheterline (36) and later supported by other researchers (35,37,38), can be qualitatively explained by a large value for r_{Pie}. Indeed, the observed decrease in A_c requires 1), that dissociation of Mg-ADP-Pi-actin from the filament ends is very slow relative to Mg-ADP-actin as previously documented (35,38), and 2), a substantial fraction of the actin filament end with ADP-actin in the absence of Pi. In the absence of a large value for r_{Pie}, our model predicts that the number of filaments with ADP-subunit ends is very small (0.8% for the barbed end and 7.6% for the pointed end), and our model therefore provides additional quantitative evidence that $r_{Pie} \gg 1$.

Fig. 5 demonstrates the dependence of A_c on phosphate concentration [Pi] for the barbed and pointed ends in the absence of profilin calculated with the parameters specified in Table 2. Note that for the pointed end there are two sets of k_{T-} and k_{T+} values in Table 2 based on different assumptions discussed below. The different assumptions are shown in Fig. 5 to have little effect on A_c.

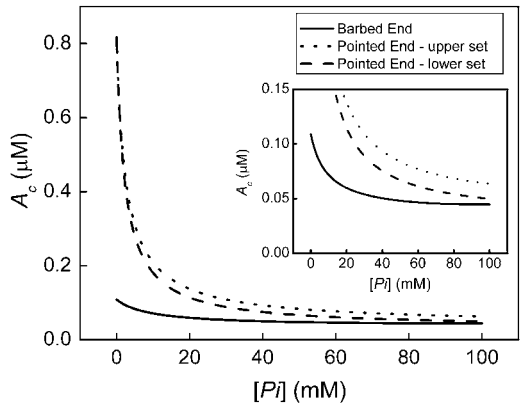

FIGURE 5 Dependence of A_c on inorganic phosphate concentration. Dependence of A_c on inorganic phosphate concentration [Pi] is calculated according to the complete set of the analytical equations derived in part 2 of Appendix 1 with the parameters specified in Table 2. (*Inset*) The same plots on an expanded scale for low values of A_c. The designations ''upper set'' and ''lower set'' refer to the parameter set in Table 2 for which either published values for the pointed-end association and dissociation rate constants (32) or detailed energy balance, respectively, are utilized in the calculation.

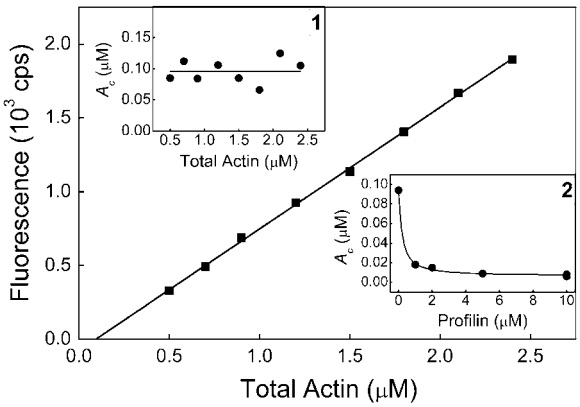

FIGURE 6 ADP-ATP exchange of G-actin at steady state is unlikely to be a rate-limiting step in the absence of profilin. Actin critical concentration measured with pyrene actin fluorescence technique (*squares*) and with fluorescent anisotropy technique (*inset 1*, *circles*). The first technique provides the difference between total and filamentous actin, which includes both ATP-bound and ADP-bound G-actin forms. According to this technique, $A_c = 0.093 \pm 0.016$ μM. The second technique is sensitive only to ATP-bound G-actin since the affinity of thymosin β_4 to ADP-bound actin is much lower than it is to ATP-bound actin (see Experimental procedure). This method yields $A_c = 0.096 \pm 0.007$ μM. (*Inset 2*) Effect of profilin on A_c at the same conditions measured with the fluorescent anisotropy technique as described in ''Experimental procedure''.

Actin steady-state dynamics in the presence of profilin

Mechanism II: acceleration of ADP-ATP exchange by G-actin

As described in the Introduction, this mechanism is based on the assumption that ATP hydrolysis by actin filaments produces ADP-bound monomers faster than they exchange ADP for ATP. Therefore, monomeric ADP-bound actin accumulates at steady state. Since ADP-actin has a higher critical concentration than ATP-actin, this leads to higher A_c (15,16). Then acceleration of nucleotide exchange by profilin (11) may lead to the decrease in A_c.

However, experimental evidence supports the conclusion that nucleotide exchange is not rate limiting in the absence of profilin (15). Note also that since this effect is related to G-actin nucleotide exchange and is not related to the ability of profilin-actin complex to add to the filament end, this mechanism would lead to the expectation that profilin should be effective in decreasing critical concentration for both ends, barbed and pointed. In contrast, it is well documented that profilin cannot change A_c for actin filaments with gelsolin-capped barbed ends (4,7). In addition, an experiment shown in Fig. 6 demonstrates that in the absence of profilin there is no significant accumulation of the ADP-bound actin at steady state. At the same conditions, profilin has a significant effect on A_c (Fig. 6, *inset 2*; see also Yarmola and Bubb (4)). Thus the acceleration of ADP-ATP exchange of G-actin is unlikely the main mechanism of the effect of profilin on A_c, although this mechanism may create an additional effect at specific conditions when the number of filament ends is relatively high (16).

Our estimates, based on published rate and equilibrium constants ((33,39), Table 2) and using published estimates of the filament length (29,30), also show there is no significant accumulation of ADP-bound monomeric actin at steady state with filamentous actin concentrations up to 3–10 μM. Therefore, the concentrations of monomeric actin forms and the values of r_n (fractions of particular nucleotide forms in total monomeric actin) are mainly defined by the affinities of nucleotide-free actin to ATP and ADP, and the affinity of Pi to monomeric ADP-actin according to Eqs. A82–A85 in Appendix 1. Then with the nucleotide concentrations and parameter values specified in Table 2,

$$r_A \approx r_I \ll r_D \ll r_T \approx 1 \tag{9}$$

at 100 μM (as in Table 2) of inorganic phosphate (Pi), and

$$r_A \ll r_D \approx r_I \ll r_T \approx 1 \tag{10}$$

at 100 mM Pi, which means that the ATP-bound form is the predominant form of monomeric actin in excess ATP, consistent with our experimental results (Fig. 6). With no contribution from mechanism II, the values of r_n in Eq. 1 do not depend on profilin concentration due to detailed balance for monomeric forms (see Fig. 3), and the coefficients U_n define all the dependence of A_c on P.

For further analysis, it is useful to disregard the possible relevance of mechanism II. No assumption regarding mechanism II is necessary to evaluate mechanism III. To estimate mechanisms IV and V theoretically, we will employ the assumption that mechanism II is inactive and that monomeric nucleotide exchange is fast enough that concentrations of

monomeric actin forms are defined by Eqs. A82–A85 in Appendix 1.

Mechanism III: Destabilization of ATP and ADP binding to nucleotide-free G-actin induced by profilin

Kinosian et al. (2) proposed that profilin alters the affinity of nucleotides for actin to cause a lower A_{cb} in the presence of profilin. The differences in affinity when profilin is either bound or unbound are shown in Fig. 3 as a potential difference between K'_{dATP} and K_{dATP} and a potential difference between K'_{dADP} and K_{dADP}. Mechanism III can be evaluated in our model by setting the rates of ATP hydrolysis and phosphate release to zero in the final analytical expressions. Part 3 of Appendix 2 considers a limiting case when there is no ATP hydrolysis by F- or G-actin and no phosphate binding and release by F-actin. It is shown there that at these conditions all coefficients $U_n = 1$ in the presence and absence of profilin and the A_c is defined by (see Eq. B31)

$$A_c^{-1} = \sum r_n \times A_{cn}^{-1}. \tag{11}$$

The conclusion for ADP actin is the same since it follows automatically from the same equation by setting the ATP concentration to zero.

Mechanism II is always inactive in the absence of ATP hydrolysis by polymeric and monomeric actin. In addition, the affinities of profilin to different nucleotide forms of G-actin and the affinities of ATP and ADP to free actin and profilin-actin must satisfy detailed thermodynamic balance, and therefore the values of r_n cannot be affected by the presence of profilin. Parameters A_{cn} do not depend on profilin concentration. Then, none of the terms in Eq. 11 depends on profilin concentration, and therefore A_c is the same at any profilin concentration. This means that mechanism III is not possible at steady state. This result is expected theoretically since in the absence of ATP hydrolysis there is no energy source to support the misbalance of the apparent energy square related to the profilin pathway. The conclusion that profilin can influence A_{cb} without ATP hydrolysis results from considering differences in actin nucleotide affinities caused by profilin without taking into account the corresponding differences in profilin affinity for actin (see Fig. 3, ''detailed balance for monomeric actin forms'' for correct relationships). Instead, K_{dT}, K_{dD}, and K_{dA} are all referred to as K_{PA} (2).

Nucleotide identities of the filament tips and independence of nucleotide forms in the absence of ATP hydrolysis

As derived in part 3 of Appendix 2 (Eqs. B39 and B40), the fractions of the of the uncapped filament ends bound to a certain nucleotide type $g_n = g_{n(1)}/g_f$ (see definitions in Table 1) in the absence of ATP hydrolysis

$$g_n = r_n \times A_c \times A_{cn}^{-1}, \tag{12}$$

and therefore Eq. 1 becomes equivalent to the statement that

$$\sum g_n = 1. \tag{13}$$

Note that even is this simple case the filament tip nucleotide states are not the same as the monomer nucleotide states: $g_n \neq r_n$ in the presence or absence of profilin. Moreover, from Eq. 12, it follows that the rate of polymerization $k_{ON(n)}$ for each individual form n is equal to the rate of depolymerization $k_{OFF(n)}$ for this form (including subunits bound to profilin):

$$k_{ON(n)} = k_{OFF(n)}, \tag{14}$$

where

$$k_{ON(n)} = g_f \times r_n \times A_c \times S_n \times k_{n+} \tag{15}$$

$$k_{OFF(n)} = g_{n(1)} \times S_n \times k_{n-} \tag{16}$$

(see Eqs. A5–A7, A21, and A22 in Appendix 1). Coefficients S_n in Eqs. 15 and 16 are factors that define the acceleration of polymerization and depolymerization rates by profilin for the corresponding nucleotide form. They are discussed in more detail in the subsection ''Affinity mechanism (IVb)''. In the absence of profilin, $S_n = 1$. Eq. 14 means that since in the absence of ATP hydrolysis and phosphate binding and release by filamentous actin there is no interconversion between forms in polymeric actin, then at steady state the number of binding events for each form should be equal to the number of the depolymerization events for this form. Therefore, all forms polymerize and depolymerize independently of each other and there is no flux in the monomeric nucleotide exchange since there is no net supply of different monomeric forms by polymeric actin.

The rate of exchange diffusion and the physical meaning of coefficients U_n

If ATP hydrolysis is present, there is no simple relation between the terms in Eq. 1, g_n and U_n for $n = T, I,$ or D. Eq. 1 can be rewritten as

$$\sum g_n \times U_n^{-1} \times k_{ON(n)}/k_{OFF(n)} = 1, \tag{17}$$

where $k_{ON(n)}$ and $k_{OFF(n)}$ are defined by Eqs. 15 and 16. Still $g_A = r_A \times A_c \times A_{cA}^{-1}$, $k_{ON(A)} = k_{OFF(A)}$ and $U_A = 1$ because the nucleotide-free form does not convert to other forms in filamentous actin in the presence or absence of ATP hydrolysis. The other terms in Eqs. 1 and 17 are no longer independent: $k_{ON(n)} \neq k_{OFF(n)}$ and coefficients $U_n \neq 1$ for $n \neq A$ in the presence or absence of profilin. Note also that $k_{ON(n)}/k_{OFF(n)} \neq U_n$. Equations 1 and 17 are not, in general, equivalent to Eq. 13. Although since ATP hydrolysis is modeled here as an irreversible reaction, the ATP-bound form is relatively independent. One obtains for g_T (see Eqs. A78 and A60 in part 2 of Appendix 1)

$$g_T = r_T \times A_c \times A_{cT}^{-1} \times (1 + e)^{-1}, \tag{18}$$

where

$$e = \alpha \times k_H/(S_T \times k_{T-}) = k_{HYD}/k_{OFF(T)}, \quad (19)$$

where α is defined by Eq. A63.

As shown in part 2 of Appendix 2 (Eqs. B28 and B29), variable α in Eq. 19 is related to an average length of the filament's ATP cap, L_{Cap}, which in turn is equal to the sum of probabilities for all subunits in the filament to carry ATP. The value of $k_{HYD} = \alpha \times k_H \times g_{T(1)}$ is the total rate of hydrolysis per filament, and $\alpha \times g_{T(1)}$ is the length of the ATP cap in the absence of profilin or in the case when profilin is present and does not accelerate ATP hydrolysis (see Eq. B29 in part 2 of Appendix 2). From Eqs. 15, 16, 18, and 19, it follows that

$$(1 + e) = k_{ON(T)}/k_{OFF(T)}, \quad (20)$$

and naturally,

$$k_{ON(T)} = k_{HYD} + k_{OFF(T)}. \quad (21)$$

Note that the variable e, which is the ratio of the net rate of hydrolysis per filament to the net rate of depolymerization of the ATP-carrying subunits from the filament end, defines the fate of the ATP-bound subunits inside the actin filament. Indeed, at steady state, an ATP-bound polymeric subunit has two final possibilities: either to undergo hydrolysis (and depolymerize) or to depolymerize as the ATP-bound (T) subunit. Note that $k_{OFF(T)}$ is the rate at which that latter event occurs, that of simple cycling of the T subunits between polymeric and monomeric states without conversion to other forms or, effectively, the rate of the exchange of T subunits for T subunits. The hydrolysis rate per filament, $k_{HYD} = k_{ON(T)} - k_{OFF(T)}$ is the rate of the former event. Thus k_{HYD} is, in fact, equal to the rate of exchange diffusion in the absence of treadmilling. Indeed, this is the net rate of the cycling for the subunits that bind to the filament tip as form T, undergo hydrolysis with subsequent depolymerization, and after the exchange of ADP for ATP are ready for the next cycle (see Fig. 2). Therefore $e = k_{HYD}/k_{OFF(T)}$ is equal to the ratio of the rate of the exchange diffusion (the rate of the exchange of T subunits for D subunits in the actin filament) to the rate of depolymerization of T subunits (the exchange of T subunits for T subunits). We call the variable e the ''exchange diffusion ratio''.

Note that even though the hydrolysis rate per filament equals the rate of exchange diffusion, this does not negate the observation that hydrolysis and exchange diffusion, in general, have opposite effects on A_c. In the absence of exchange diffusion, hydrolysis alone would drive the critical concentration toward A_{cD}, and the occurrence of exchange diffusion brings this value back toward A_{cT}.

When the ATP-bound form is predominant in the monomeric actin pool (see Eqs. 9 and 10), Eq. 1 reduces to Eq. 2 and the steady-state flux of subunit exchange E (see Eqs. A5–A7, A21, and A22 in Appendix 1)

$$E = k_{ON} = k_{ON(T)} = g_f \times S_T \times k_{T+} \times A_c = g_f \times S_T \times k_{T-} \times U_T \quad (22)$$

$$E = k_{OFF} = \sum k_{OFF(n)} = \sum g_{n(1)} \times S_n \times k_{n-}. \quad (23)$$

Then

$$U_T = k_{OFF}/(g_f \times S_T \times k_{T-}) = \sum g_n \times (S_n \times k_{n-})/(S_T \times k_{T-}). \quad (24)$$

Thus, at conditions when all monomeric actin is ATP bound (although not in the general case), U_T is the normalized net rate of depolymerization which corrects for the effect of the conversion of the ATP-bound form to other forms with different depolymerization rate constants. Note that since U_T is normalized by the acceleration factor S_T and the capping factor g_f, it does not directly reflect the enhancement of the polymerizing monomer concentration due to the presence of actin-profilin complex, but rather reflects the effect of profilin on the way in which the forms convert to each other. When hydrolysis is present, $U_n \neq 1$ for $n \neq A$ in the absence or presence of profilin.

Useful simplifications and key variables related to physical interpretation of mechanisms

As discussed above, with the nucleotide concentrations and parameter values specified in Table 2, the ATP-bound form is predominant in the G-actin monomeric pool. Then Eq. 1 reduces to Eq. 2 and in the absence of the mechanism II, function U_T completely defines dependence of A_c on profilin concentration P at these conditions. For further analysis and physical interpretation of the resulting analytical equations obtained in part 2 of Appendix 1, it is useful to note the following. According to published data, the rate of Pi release by interior ADP-Pi-carrying filamentous subunits k_{Pi-} is ~100 times slower that the rate of ATP hydrolysis k_H, and the rate of Pi binding by these subunits $k_{Pi+} \times [Pi] \ll k_{Pi-}$ at 100 μM of Pi. In addition, recent work of Fujiwara et al. discussed earlier in this manuscript suggests that $r_{Pie} = k_{Pie-}/k_{Pi-} \approx 8000 \gg k_H/k_{Pi-}$ (35) where k_{Pie-} is the rate of Pi release by the ADP-Pi-carrying subunits at the filament end (see Fig. 3 for parameter definitions). Taking this into account, one obtains (see Eqs. B22 and B26 derived in part 2 of Appendix 2)

$$U_T \approx (1 + e)/(1 + d \times e) \quad (25)$$

$$g_T = (1 + d \times e)^{-1} \quad (26)$$

$$g_Y \approx 1 - g_T, \quad (27)$$

where e is defined by Eq. 19, and

$$d = (S_T \times k_{T-})/(S_Y \times k_{Y-}). \quad (28)$$

As before, index Y stands for either I or D. $Y = D$ is applicable for low (100 μM or less) and $Y = I$ for high (50–100 mM) Pi concentrations. At these conditions, only two nucleotide forms at the filament tip are prevalent: T and either I or D, depending on Pi concentration.

Appendix 2 provides a detailed analysis of the limiting cases discussed here. As discussed above, part 1 of Appendix 2 considers the hypothetical case when ATP hydrolysis and phosphate release are both very fast compared to the subunit exchange. Part 2 considers the case when the rate of hydrolysis is comparable to the rate of subunit exchange and either i), parameters for ADP and ADP-Pi actin forms are the same or overall phosphate release is very slow compared to hydrolysis, or ii), overall phosphate release is very fast compared to hydrolysis. Part 3 considers the case in which there is no ATP hydrolysis by F- or G-actin and no phosphate binding and release by F-actin. Part 1 and the limiting case (i) in part 2 provide a comparison of our model with models developed by others. The limiting case (ii) in part 2 corresponds to the set of parameters shown in Table 2. Part 3 is used to evaluate mechanism III.

A result similar to the combination of Eqs. 2, 19, 25, and 28 (with $S_n = 1$, see Eq. B27), was obtained by Stukalin and Kolomeisky with a stochastic model for actin polymerization (in the absence of profilin and with one-step hydrolysis-phosphate release) that calculates fluctuations of the filament length and of the ATP cap (40) as well as A_c. As mentioned above, our model places no limitations on the filament length distribution even though it does not calculate it.

As we discussed above, variable e is the ratio of the rate of exchange diffusion to the rate of ATP-bound subunits exchange (see Eq. 19), and therefore we call it the ''exchange diffusion ratio''. The variable d is the ratio of the rates of depolymerization for ATP- and ADP- (or ADP-Pi-) carrying ends. We will call the variable d the ''depolymerization rates ratio''. Profilin can affect U_T through its effect on both the depolymerization rates ratio (d) and the exchange diffusion ratio (e), correspondingly described as an affinity mechanism (IVb) and an acceleration mechanism (V). We will discuss these mechanisms in detail in the next sections.

Mechanism IV based on the difference in affinity of profilin to ATP- and ADP-Pi-bound barbed ends

As discussed above, in the absence of ATP hydrolysis, the apparent energy square is balanced, and A_c should remain constant at any profilin concentration. Thus, ATP hydrolysis is a necessary element in the effect of profilin on A_c. A general idea of ATP hydrolysis energy coupling to the profilin pathway was first suggested by Pantaloni and Carlier (7) and further developed in subsequent works (15,17–19). A variation of this mechanism has also been developed in Dickinson et al. (20,21). As described in the Introduction, this mechanism assumes direct incorporation of the ATP hydrolysis energy into the profilin-related pathway pg (Fig. 1) and the apparent energy square misbalance. According to this mechanism, in the profilin-related pathway pg the profilin-actin complex binds to the barbed end of actin filament with subsequent dissociation of profilin from the filament tip due to the loss of affinity resulting from ATP hydrolysis. After profilin dissociation, the actin filament is one subunit longer, and profilin can start the next cycle.

Pantaloni and Carlier (17) proposed that actin filament growth from profilin-actin complex and ATP hydrolysis are tightly coupled, i.e., the transformation of chemical energy of ATP hydrolysis into polymerization energy is regulated by the direct association of each step in the hydrolysis reaction with a corresponding step in polymerization. Thus, ATP hydrolysis should be a rate-limiting step in barbed-end polymerization in the presence of profilin (17). Acceleration of ATP hydrolysis by profilin has been suggested (17,19) so that polymerization rates can correspond to in vivo observations. This, however, does not circumvent the additional problem created by experimental evidence obtained by Blanchoin and Pollard, showing that with profilin present, hydrolysis may lag far behind polymerization (41). Such a finding contradicts any hypothesis that relies upon directly coupled ATP hydrolysis. In addition, this model adheres to the common practice of neglecting the depolymerization term involving PA dissociation from F-actin (13,21,24), the absolute value of which, as shown in Yarmola and Bubb (4), may be significantly larger than the other terms combined. Neglecting this term then leads to the false expectation of a slower net depolymerization rate and misleadingly leads to the conclusion that an explanation for lower A_c has been discovered.

Affinity mechanism (IVb)

Despite the problems described above with mechanism IV suggested by Pantaloni and Carlier, a mechanism based on the difference in the profilin affinities to different nucleotide forms of actin may exist. This effect is related to the fact that capping by profilin leads to a change in the depolymerization rate's ratio d. Due to thermodynamic constraints, the impact of the affinity mechanism on A_c is a combination of acceleration factors and differences in the affinities. It is not sensitive to the difference in the profilin affinities to the ADP- or ADP-Pi- and ATP-bound filament tips alone. As we show below, the effect of the addition of subunits due to the loss of profilin affinity to the end is compensated for by the effect of the loss of subunits due to the increased depolymerization rate of the profilin-capped end. Instead, it is the depolymerization rates ratio, which accounts for both effects and defines the outcome. For practical purposes, this effect can be much better described in terms of profilin affinity to monomeric actin forms than in terms of its affinity to the filament tips, although these affinities are of course related by the balanced thermodynamic energy squares of Fig. 1.

Indeed, one can see from Eqs. 2 and 25 that A_c should decrease with the increase of the depolymerization rates ratio d. According to its definition (see Eq. 28),

$$d = (S_T \times k_{T-})/(S_Y \times k_{Y-}) = d_0 \times S_T/S_Y, \quad (29)$$

where

$$d_0 = k_{T-}/k_{Y-}, \quad (30)$$

and coefficients S_n ($n = T$ or Y) are the factors that define acceleration of polymerization and depolymerization rates by profilin for the corresponding nucleotide form. They are equal to (see Eq. A22 in Appendix 1)

$$S_n = 1 + r_{n+} \times P/K_{dn} = 1 + r_{n-} \times P/K_{dbn}, \quad (31)$$

where r_{n+} and r_{n-} are the ratios of the rate constants for the addition (index ''+'') or dissociation (index ''−'') of profilin-actin complex and pure actin monomer of a corresponding type to (or from) the barbed end. K_{dn} and K_{dbn} are the affinities of profilin to the corresponding forms of monomeric actin or filament tips, correspondingly (see Fig. 3 for definition of parameters). The thermodynamic constraint $\Phi_n = ((r_{n+}/K_{dn})/(r_{n-}/K_{dbn})) = 1$ is used in Eq. 31 (see Eq. A1 and Figs. 1 and 3).

Experimental data suggest that r_{n+} are equal or close to 1 (2,9,17,41,42). The ratios r_{n-} are often assigned to be equal to 1 (see, for example, Romero et al. (13)), although this is not possible for any pure form if the affinities K_{dbn} and K_{dn} are different, and $r_{n+} \approx 1$. Indeed, according to Eq. A1 in Appendix 1 (see also Figs. 1 and 3),

$$r_{n-} = r_{n+} \times K_{dbn}/K_{dn} \approx K_{dbn}/K_{dn}, \quad (32)$$

and r_{n-} could be in the range of 20–1000 (2,4,9,14).

At saturation with profilin,

$$d_{sat} = d_0 \times S_T/S_Y \approx d_0 \times (K_{dbY}/K_{dbT}) \times (r_{T-}/r_{Y-}) = d_0 \times K_{dY}/K_{dT} \times (r_{T+}/r_{Y+}) \approx d_0 \times K_{dY}/K_{dT}. \quad (33)$$

If the affinity of profilin to ADP or ADP-Pi G-actin is lower than that to ATP-G-actin, profilin should increase d, thus decreasing A_c (see Eqs. 2 and 25). This effect is demonstrated in Fig. 7 (*A*, *C*, and *D*, *red curves*). The ratio r_{T+}/r_{D+} can also add to the described effect. According to the experimental data (2,9,17,41,42), $r_{T+} = 0.6$–1.0, and $r_{D+} = 0.5$–0.8. We will call the affinity mechanism described here ''mechanism IVb'' to distinguish it from the ''mechanism IV'' suggested by Pantaloni and Carlier.

Differences between mechanisms IVb and IV

The affinity mechanism described here is similar to the above mentioned mechanism IV suggested by Pantaloni and Carlier, although there are important differences between the two mechanisms:

a. Hydrolysis of ATP is a rate-limiting step in the mechanism by Pantaloni and Carlier (17). Our affinity mechanism is based on indirect coupling and places no temporal restriction on ATP hydrolysis. ATP hydrolysis may lag behind actin polymerization, consistent with experimental data (41).
b. Pantaloni and Carlier proposed that the energy incorporation occurs through the loss of profilin affinity to the barbed end when the ATP-carrying end subunit undergoes hydrolysis, i.e., their mechanism is based on the difference of the profilin affinities to the filament tips K_{dbT} and K_{dbI}. Although due to thermodynamic constraints, A_c is not sensitive to the difference in K_{dbT} and K_{dbI} alone since the effect of the addition of subunits due to the loss of profilin affinity to the end (K_{dbY}/K_{dbT}) is compensated for by the effect of the increased depolymerization rate of the profilin-capped end (r_{Y-}/r_{T-}), which is often neglected (13,21,24). As explained above, for practical purposes this effect is much better described in terms of K_{dY} and K_{dT} rather than K_{dbY} and K_{dbT}. If d_{sat} is expressed in terms of K_{dbY}/K_{dbT}, there is an uncertain factor of r_{T-}/r_{Y-}, which could be a number much larger or much smaller than 1.
c. Mechanism IV proposed by Pantaloni and Carlier is based on the difference in the interaction of profilin with ADP-Pi and ATP forms and relies on the assumption that phosphate release from the ADP-Pi subunit at the filament end is slow (see Gutsche-Perelroizen et al. (17)). New experimental evidence (35) (supported by our results) suggests that the value of r_{Pie} is likely very large, and therefore, overall release of Pi is fast. Then the percentage of ADP-Pi bound subunits at the barbed end $g_{I(1)}$ should be very small in the absence and presence of profilin unless profilin very significantly accelerates ATP hydrolysis (see nucleotide profiles on Fig. 9). Our calculations show that with the parameters as in Table 2 and acceleration of hydrolysis by profilin by a factor of 1000, $g_{I(1)}$ only increase from 3% to 30% at 20 μM free profilin, although $g_{D(1)}$ increases from 11% to 66%. Another means to increase $g_{I(1)}$ is for profilin to cause a significant decrease in the rate of Pi release ($r_{Pi} \ll 1$) and this seems unlikely.

Mechanism IVb can turn hydrolysis from a factor working against polymerization to a factor that promotes polymerization

It is important to note that from Eq. 25, it directly follows that

$$\text{Case A. } U_T \geq 1 \text{ and } A_c \geq A_{cT} \text{ when } d \leq 1, \text{ and} \quad (34)$$

$$\text{Case B. } U_T \leq 1 \text{ and } A_c \leq A_{cT} \text{ when } d \geq 1. \quad (35)$$

These two cases correspond to cases A and B discussed above in the section ''Actin steady-state dynamics in the absence of profilin''. Indeed, in the absence of profilin $d = d_0 = k_{T-}/k_{Y-}$ (see Eq. 30). Note that if mechanism IVb exists and $K_{dY}/K_{dT} >$

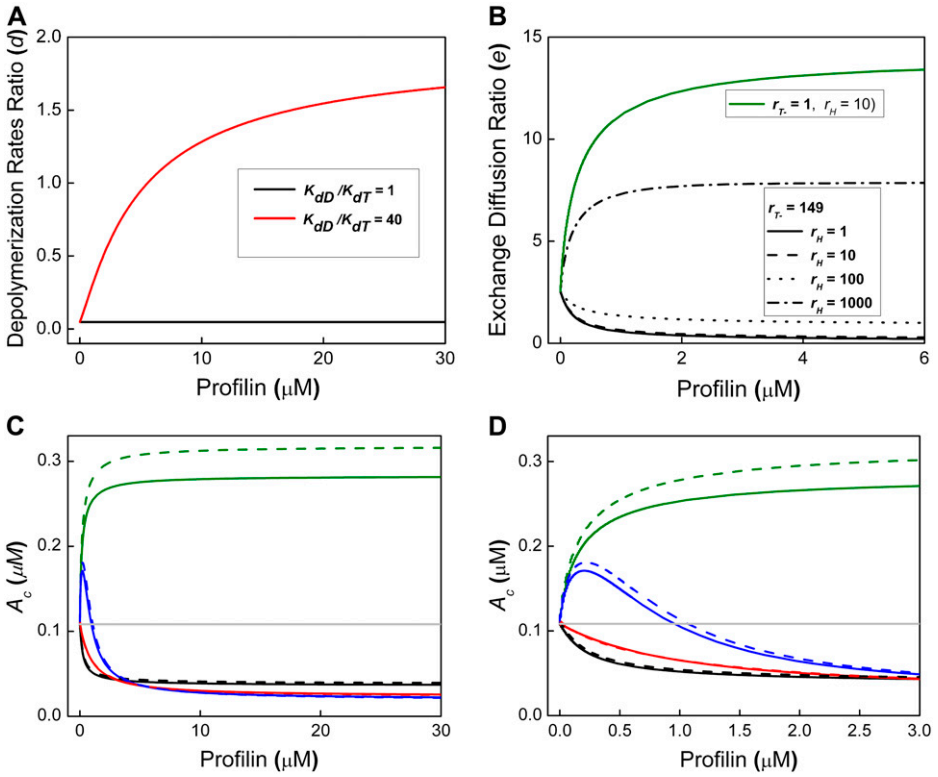

FIGURE 7 Illustration to the explanation of mechanisms V and IVb. Dependence of key variables and actin critical concentration on profilin concentration for different parameter sets, each corresponding to a specific mechanism and/or effect. Parameters are specified in Table 2 with the following changes: for all sets $r_{n+} = 1$, for all $n \neq D$ $K_{dn} = 0.1$ μM, plus specific changes for each set described below. (*A* and *B*) Depolymerization rates ratio (*A*) and the exchange diffusion ratio (*B*) calculated with the following specific parameter changes: (*A*) Black curve: $K_{dD} = 0.1$ μM $= K_{dT}$ (depolymerization rates ratio $d = d_0$); red curve: $K_{dD} = 4.0$ μM $= 40 \times K_{dT}$ ($d_{Sat} = 40 \times d_0$); (*B*) Green curve: $K_{dD} = 0.1$ μM, all $K_{dbn} = 0.1$ μM and therefore $r_{n-} = 1$, and $r_H = 10 > r_{n-}$; (effect of the acceleration of ATP hydrolysis alone); black curves: $K_{dD} = 0.1$ μM, $K_{dbn} = 14.9$ μM (as in Table 2) and therefore $r_{n-} = 149$ and $r_H = 1$ (*solid line*), $r_H = 10$ (*dashed line*); $r_H = 100$ (*dotted line*); $r_H = 1000$ (*dash-dot line*); (exchange diffusion with the acceleration of ATP hydrolysis). (*C* and *D*) Critical concentration A_c at high (*C*) and low (*D*) profilin concentrations for different parameter sets, each corresponding to the specific mechanism and/or effect. All solid curves are calculated for the barbed end according to the complete set of the analytical equations derived in part 2 of Appendix 1 with the parameters specified in Table 2 with the following changes: for all sets all $r_{n+} = 1$, for all $n \neq D$: $K_{dn} = 0.1$ μM, and black curves: $K_{dD} = 0.1$ μM (set corresponds to the acceleration mechanism (V) alone); Red curves, $K_{dD} = K_{dbD} = 4.0$ μM $= 40 \times K_{dT}$, and for all $n \neq D$ $K_{dbn} = 0.1$ μM (affinity mechanism (IVb) alone); Green curves: $K_{dD} = 0.1$ μM, all $K_{dbn} = 0.1$ μM, and $r_H = 10$ (effect of the acceleration of ATP hydrolysis alone); Blue curves: $K_{dD} = K_{dbD} = 4.0$ μM, for all $n \neq D$ $K_{dbn} = 0.1$ μM and $r_H = 10$ (affinity mechanism (IVb) combined with the effect of acceleration of ATP hydrolysis). Gray flat line: $K_{dn} = K_{dbn} = 0.1$ μM, $r_H = 1$ (no mechanisms). The dashed curves are calculated for the same parameter sets according to simplified analytical equations (Eqs. 2, 19, 25, and 28). There is no significant difference between the curves calculated according to the simplified and full sets of equations.

d_0^{-1}, profilin may convert the described above case A ($d_0 \leq 1$) to the case B ($d_{sat} \approx d_0 \times K_{dY}/K_{dT} > 1$) and turn hydrolysis from a factor working against polymerization to a factor that promotes polymerization, according to prevailing assumptions.

Acceleration of ATP hydrolysis may multiply the effect of the affinity mechanism (IVb)

Note that the effect of the depolymerization rates ratio d on U_T in the affinity mechanism IVb depends on the exchange diffusion ratio e. When $e < 1$, the effect of d on U_T is very limited (see Eq. 25). If e increases, the effect of profilin on A_c through the affinity mechanism IVb could be multiplied. In case A ($d < 1$), the larger the e, the larger the A_c. Although if the above described affinity mechanism turns case A to case B ($d > 1$), A_c should decrease with the increase of e. In the limit, when $e \gg 1$, $U_T = d^{-1}$, and at saturation with profilin $A_c \approx A_{cT} \times (k_{Y-} \times K_{dT})/(k_{T-} \times K_{dY})$ and may theoretically become much smaller than A_{cT} (see Eqs. 2, 25, and 33). Indeed, the exchange diffusion ratio e can be separated into two components, variable $h \times s$ and variable l (see Eqs. A63 and A66):

$$e = h \times s + l \tag{36}$$

where

$$l = (\lambda/(1-\lambda)) \times k_H/(g_f \times S_T \times k_{T-}) \tag{37}$$

$$h = k_H/k_{T-} \tag{38}$$

$$s = S_H/S_T \tag{39}$$

$$S_H = r_{He} \times (1 + r_H \times P/K_{dbT}). \tag{40}$$

Variable $h \times s$ in Eq. 36 is related to acceleration of ATP hydrolysis by the filament end subunit bound to profilin (17) which is characterized by parameter r_H (see Fig. 3 for definition). Parameter h in Eqs. 36 and 38 does not depend on P. Variable s may increase or decrease with increasing profilin concentration, and at saturation with profilin (see Eqs. 31, 32, 39, and 40)

$$s_{sat} = r_{He} \times r_H/r_{T-}. \tag{41}$$

Since, as stated above, r_{T-} could be in the range of 20–1000, acceleration of ATP hydrolysis by profilin must be very

significant ($r_H > r_{T-} \approx 20$–1000) to increase the value of s and hence e.

The effect of the acceleration of ATP hydrolysis on the exchange diffusion ratio e is shown in Fig. 7 *B*. Black curves show the dependence of e on profilin concentration for several values of r_H with $r_{T-} = 149$ (corresponding to the parameter set in Table 2), and the green curve shows the effect of r_H with a hypothetical value of $r_{T-} = 1$, which is used to eliminate the effect of the acceleration of exchange diffusion (see discussion below). Note that since the effect of the acceleration of ATP hydrolysis on e depends on the ratio r_H/r_{T-}, the same value of $r_H = 10$ produces opposite effects on e with different values of r_{T-} (compare the *green curve* with the *dashed black curve* in *panel B*). The effect of the acceleration of ATP hydrolysis on A_c is shown in Fig. 7, *C* and *D*. Green curves show the effect of acceleration of hydrolysis alone, and blue curves show this effect in combination with the affinity mechanism.

Mechanism V based on acceleration of the process of exchange diffusion by profilin

As illustrated by Fig. 4, the faster the hydrolysis compared to the subunit exchange, the more filament ends become ADP-bound. Since for the barbed end, ADP-bound subunits dissociate faster, ATP hydrolysis leads to $A_c > A_{cT}$ in the absence of profilin. Profilin accelerates the polymeric subunits exchange, attenuating the effect of ATP hydrolysis and bringing A_c closer to A_{cT}.

As discussed above, the exchange diffusion ratio e is the ratio of the rate of exchange diffusion to the rate of the exchange of the *T*-type subunits that do not undergo conversion to other forms but simply cycle between monomeric and polymeric states (Eq. 19). When *D*- and *I*-ends depolymerize faster than *T*-ends (case A, $d < 1$, $U_T > 1$), profilin decreases A_c by decreasing e and therefore bringing U_T closer to 1. As shown above (see Eqs. 36–39), the effect of profilin on e consists of two effects: acceleration of ATP hydrolysis and acceleration of the overall subunit exchange. These two processes produce opposite effects on the nucleotide profile and A_c. Variable l in Eqs. 36 and 37 decreases with an increase of P due to the acceleration of the subunit exchange. Even though the rate of exchange diffusion itself increases with profilin concentration because of the increased supply of polymerizing *T*-subunits, it is limited by the rate of hydrolysis if hydrolysis is not being significantly accelerated. On the other hand, the rate of the *T*-form cycling is not limited by hydrolysis, and therefore increases faster, decreasing e. Then in the case when $r_H \leq r_{T-}$, both variables s and l and therefore e decrease with an increase of P (see Fig. 7 *B*), and U_T and A_c decrease with the decrease of e (see Fig. 7, *C* and *D*, *black curves*). When $r_H > r_{T-}$, the acceleration ATP hydrolysis by the filament end subunit caused by profilin works opposite to the effect of the acceleration of subunit exchange and at certain profilin concentration may overcome the effect of the acceleration of subunit exchange and cause e to increase with P. Although as discussed above, an increase in e can decrease A_c only when $K_{dY}/K_{dT} > d_0^{-1}$ (active mechanism IV) and P is high enough to turn $d > 1$, which may happen at higher P than the one at which an increase in e begins. Then an increase in e due to the acceleration of ATP hydrolysis increases A_c at low P and decreases it at high P (Fig. 7 *C*, *blue curve*).

The dashed curves in Fig. 7, *C* and *D*, are calculated for the same parameter sets according to simplified analytical equations with the assumption that the ATP-bound form is predominant in the monomeric pool (Eqs. 2, 19, 25, and 28). Note that there is no significant difference between the curves calculated according to the simplified (*dashed curves*) and full (*solid curves*) sets of equations. The same applies to the results shown on Fig. 8 calculated for different parameter sets corresponding to the experimentally defined parameters (see below), although the curves calculated according to the simplified equation are not shown on Fig. 8. This result justifies our analysis and explanation for the physical mechanisms V and IVb based on simplified Eqs. 2, 19 , 25, and 28.

Fig. 7, *C* and *D*, shows the effect of profilin on A_c for several parameter combinations, each corresponding to specific mechanisms: black curves show the effect of mechanism V alone, a parameter set with $r_H = K_{dD}/K_{dT} = 1$. Red curves show the affinity mechanism IVb ($K_{dD}/K_{dT} = 40$) without the acceleration of hydrolysis ($r_H = 1$) and without a significant influence of the effect of mechanism V. Green curves show the effect of the acceleration of hydrolysis ($r_H = 10$) without mechanisms IV and V, and blue curves show the acceleration of hydrolysis acting together with mechanism IVb. Note that it is not possible to completely eliminate the influence of mechanism V using specific parameter settings since the value of e is sensitive to the nucleotide identity of the end which depends on d. Of course with the setting $r_H = K_{dn}/K_{dT} = 1$ and $K_{dbn}/K_{dn} = 1$, it is possible to eliminate all mechanisms (Fig. 7, *C* and *D*, *gray flat line*).

The ratios K_{dbn}/K_{dn} mainly define the effect of mechanism V. For example, for the pure ATP form (no hydrolysis), the acceleration factor is simply equal to $r_{T-} \approx K_{dbT}/K_{dT}$ at saturation with profilin (see Eqs. 31, 32, A47, A48, and definition of g_f in Table 1). In the presence of hydrolysis, the acceleration factor is affected by other factors when $r_H \neq 1$ and/or mechanism IV is active. Note also that the parameter sets with $K_{dbn}/K_{dn} = 1$ are not realistic since it is well documented that profilin has lower affinity to the barbed end than to monomeric actin. Therefore the only parameter set in Fig. 7 that approximately corresponds to the experimentally measured parameters is the set related to mechanism V alone, represented by black curves. The parameter values reported in the literature and results obtained with these values (Figs. 8 and 9) are discussed in the next section.

DISCUSSION

Effect of parameters on model predictions

As discussed above, there are certain key parameters that define the outcome for A_c and the filament nucleotide profile

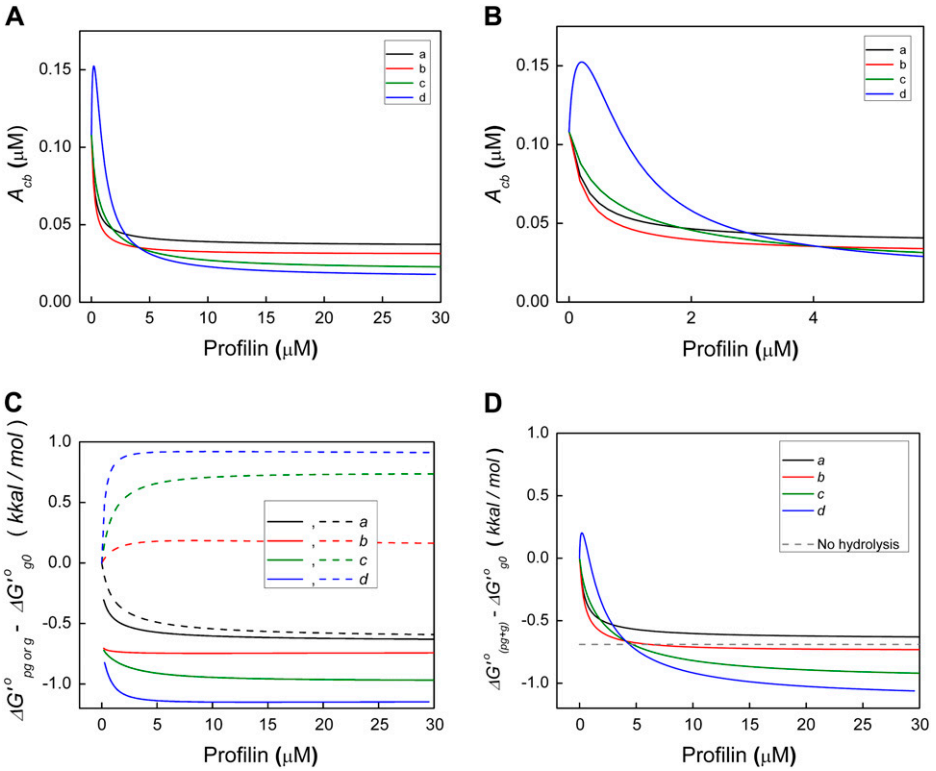

FIGURE 8 Dependence of A_{cb} on profilin concentration and comparison of the standard free energy changes for different actin polymerization pathways. (*A* and *B*) Barbed-end critical concentration A_{cb} in the presence of excess ATP and low [Pi] at high (*A*) and low (*B*) profilin concentrations. A_{cb} is calculated according to the complete set of the analytical equations derived in part 2 of Appendix 1 with the parameters specified in Table 2 with a) no changes (*black curves*, mechanism V alone); b) $K_{dD} = 4.0 = 40 \times K_{dT}$ (*red curves*, mechanisms IVb and V together); c) $K_{dD} = 4.0$ and $r_H = 100$ (*green curves*, mechanisms IVb and V plus effect of acceleration of ATP hydrolysis); d) $K_{dDI} = 4.0$ and $r_H = 1000$ (*blue curves*, same effects as in c). (*C* and *D*) Comparison of the standard free energy changes for different actin polymerization pathways. Three pathways may be compared: *pg*, *g*, and g_0, each with the corresponding standard free energy change: $\Delta G'^0_{pg}$, $\Delta G'^0_{g}$, $\Delta G'^0_{g0}$. (*C*) The differences $\Delta G'^0_{pg} - \Delta G'^0_{g0}$ (*solid lines*) and $\Delta G'^0_{g} - \Delta G'^0_{g0}$ (*dashed lines*) as functions of profilin concentration for the parameter sets *a–d* of *A* and *B*. The difference between the solid and dashed lines corresponds to the value of $\Delta G'^0_{pg} - \Delta G'^0_{g}$. (*D*) The difference $(\Delta G'^0_{(pg+g)} - \Delta G'^0_{g0}) = -RT\ln(A_{c0}/A_c)$ between the standard free energy changes for actin polymerization in the presence of profilin (through both pathways *pg* and *g*) and the pathway g_0 in the absence of profilin for the parameter sets *a–d*. In addition, *D* shows the value of $\Delta G'^0_{(pg+g)h0} - \Delta G'^0_{g0}$ for the hypothetical case of the absence of ATP hydrolysis (see Appendix 3) with a dashed gray line.

$g_{n(i)}$, and there are parameters to which the results are not sensitive. The parameter values summarized in Table 2 were taken mainly from the literature with designated references. Parameter definitions are shown in Fig. 3. Some of the parameters were obtained from thermodynamic constraints or assumed to be similar to the parameters for other actin forms when information regarding these parameters was not available from the literature and the results for A_c were not sensitive to these parameters. The key parameters, identified here for the first time to our knowledge, provide a focus for future investigations into polymerization kinetics.

Key parameters and model predictions

The effect of variation of such important parameters as r_{Pie}, K_{dn}, and r_H is discussed above and demonstrated in Figs. 5 and 7–9. As explained above, the value of k_{T+} should be approximately equal to k_{0+} in excess ATP, and $k_{T-} \neq k_{0-}$. Therefore, we assumed $k_{T+} = k_{0+}$ in Table 2. The values of k_{T-} for the barbed and pointed ends in Table 2 were obtained from the analytical solution derived in part 3 of Appendix 1 (Eq. A91) using experimental values for k_{0-} in the presence of ATP. As demonstrated above, parameters K_{dn} and r_H are key parameters related to specific mechanisms. Controversy exists in the literature regarding the specific values of these parameters. For example, experimental data regarding the affinity of profilin to different forms of G-actin are incomplete and contradictory. According to Perelroizen et al., K_{dD} is ~20 times larger than K_{dT} (43), although according to Kinosian et al., they are approximately the same (39). Information about the value of K_{dI} is absent from the literature. One can only surmise that it is intermediate between K_{bT} and K_{dD}. In Table 2, we take the parameters reported in Kinosian et al. (39) and then vary K_{dD} in Figs. 8 and 9 to demonstrate the effect of this parameter. The same applies to the value of r_H. A large acceleration of the ATP hydrolysis has been postulated in Gutsche-Perelroizen et al. (17) although there are limited experimental data supporting the acceleration (19) and there are data supporting an absence of the acceleration (41). In addition, acceleration of hydrolysis observed in Romero et al. (19) is not necessarily related to the value of $r_H > 1$ but may be related to the effect of mechanism V as discussed above. In Figs. 8 and 9, we varied r_H from 1 to 1000 to demonstrate its effect.

Fig. 8, *A* and *B*, shows the effect of profilin on A_c for several parameter combinations: *a*, the effect through the acceleration of exchange diffusion mechanism (mechanism V) alone, *b*, with the addition of the affinity mechanism IVb ($K_{dD}/K_{dT} = 40$), and *c* and *d*, with the addition of the acceleration of ATP hydrolysis 100 and 1000 times, correspondingly (multiplication of the affinity mechanism IVb). Curve *a* (parameter values as in Table 2 and very similar to

the parameter setting for Fig. 7, *C* and *D*, *black curve*) shows that exchange diffusion alone can significantly decrease A_c. The affinity mechanism IVb adds to this effect, and at high P acceleration of ATP hydrolysis multiplies the effect of mechanism IVb and further decreases A_c. However, at relatively low P large acceleration of hydrolysis causes an increase rather than decrease in A_c (curve *d*).

The value of $d \times e$ in the simplified equations (Eqs. 26 and 27) defines how profilin changes the nucleotide profile of the filament: when $d \times e$ decreases, profilin enriches the filament ends with ATP-carrying subunits through acceleration of exchange diffusion; with increasing $d \times e$, profilin drives the ends toward hydrolyzed subunits. Fig. 9 shows the nucleotide profiles for barbed and pointed ends in the absence of profilin and for the barbed end at 20 μM total profilin for the same parameter sets *a–d* as shown in Fig. 8.

Other parameters

The variation of K_{dbn} for different forms (without variation in K_{dn}) shows that A_c and the nucleotide profile are not sensitive to this parameter. The explanation for this absence of sensi-

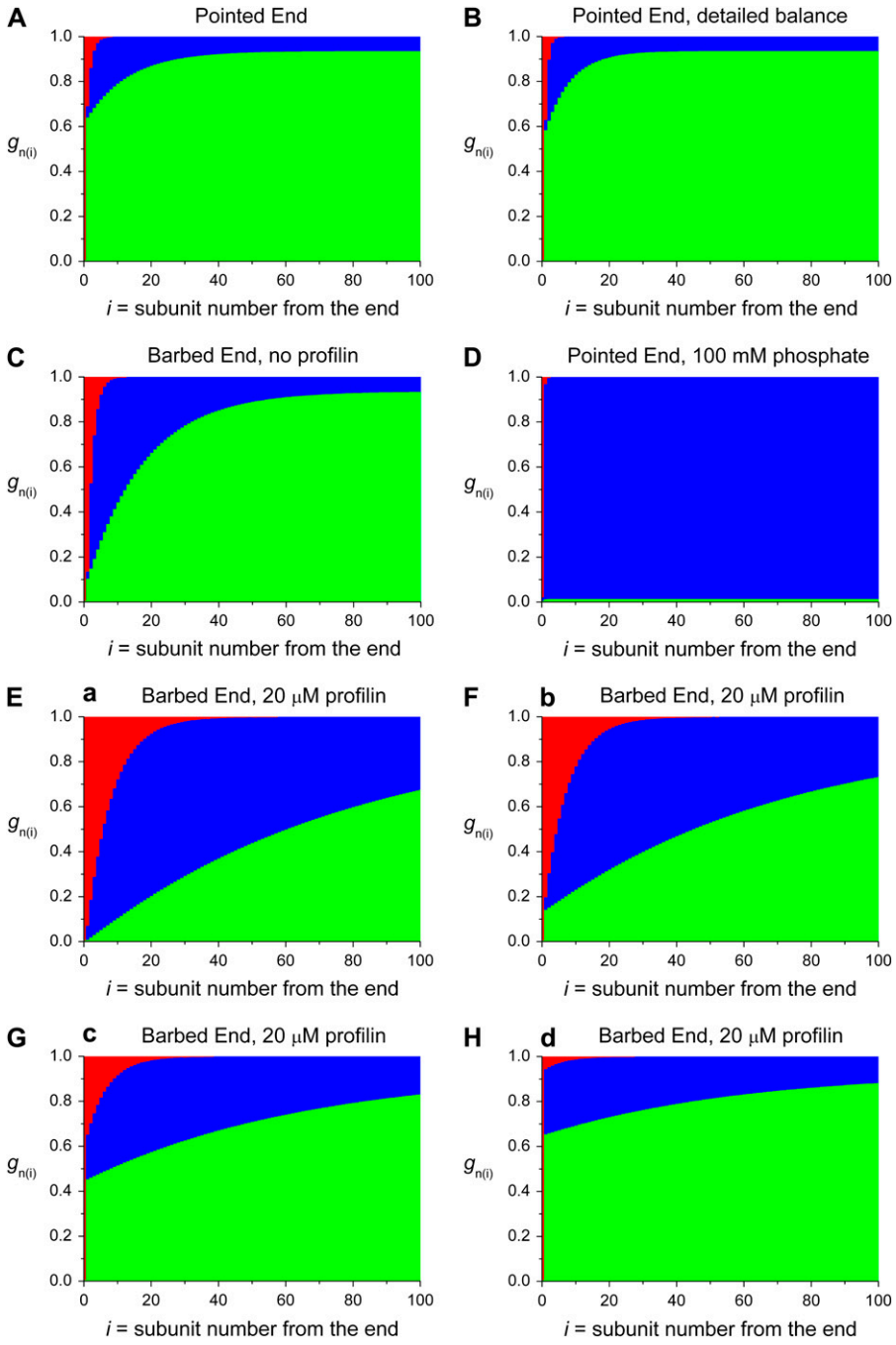

FIGURE 9 Nucleotide profiles of actin filaments. The nucleotide profiles of actin filaments $g_{n(i)}$ are shown as functions of the distance from the filament end. The distance is measured in terms of i, the number of subunits from the end, so that $i = 0$ corresponds to G-actin, and $i = 1$ corresponds to the end subunit (for $i = 1$, $g_n = g_{n(1)}/g_f$ is shown). The function $g_{T(i)}$ is shown in red, $g_{I(i)}$ is shown in blue, $g_{D(i)}$ is shown in green; $g_{A(i)}$ is negligible and therefore is not shown. The pointed-end parameters are as in Table 2. Barbed-end parameters are as in Figs. 7 and 8. The 100 μM phosphate profile for the pointed end looks identical for both pointed-end parameter sets. Panels *E–H* correspond to 20 μM of total profilin, and the parameter sets *a–d* of Fig. 8.

tivity is provided above in the discussion of the affinity-based mechanism (see Eqs. 32 and 33). Therefore, the values of K_{dbn} in Table 2 are assumed to be the same for all forms and equal to the experimentally measured (apparent) value in excess ATP. The A_c and nucleotide profile are also not sensitive to the parameters for the nucleotide-free actin form (A) since r_A is very small (see Eqs. 9 and 10) and there is no interconversion between this form and other forms inside the filaments.

Consequences of thermodynamic constraints on parameters for the pointed end

When using published experimental values of parameters, the number of constraints imposed on the system (n) is larger than the number of variables ($n-1$); thus an iterative process was used to vary the apparent rate constants k_{0+} and k_{0-} for the pointed end by a fixed factor with their ratio unchanged, with the rationale that this ratio is well-determined by prior experimental data. Then, all constraints could be satisfied without any other significant deviation from the published experimental values of parameters, with the result that k_{0+} and k_{0-} were reduced by a factor of 2.8, and their ratio unchanged with $A_{cp} = 0.79\ \mu M$ (the lower pair of values in Table 2). Alternatively, the use of published values for k_{0+} and k_{0-} (the upper pair of values in Table 2) was possible only if the constraint imposed by Eq. 6 was lifted for the pure ATP form. As stated above, the values of k_{T-} for both ends were calculated using the experimental (apparent) values for A_{c0} in the presence of ATP as derived in part 3 of Appendix 1. One can see from Figs. 5 and 9 that dependence of A_c on phosphate concentration and the filament nucleotide profiles are very similar for the two pairs of values for k_{0+} and k_{0-}.

In fact, the problem introduced by the requirement of detailed thermodynamic balance is common to all prior attempts to explain the available experimental data, although this has not been explicitly recognized. Indeed, if one assumes the values of $k_{p+} = 0.56\ s^{-1} \times \mu M^{-1}$ and $k_{p-} = 0.44\ s^{-1}$ as in Kuhn and Pollard (32), and the parameters for ADP and ATP-Pi forms as in Table 2 (35) (we do not consider here the nucleotide-free form parameters since as discussed above, the effect is negligible), the value of k_{T-} must be necessarily $\geq 0.44\ s^{-1}$ to satisfy the general rule:

$$\min(k_{n-}) \leq k_{0-} = \sum g_{n(1)} \times k_{n-} \leq \max(k_{n-}), \qquad (42)$$

where

$$0 \leq g_{n(1)} \leq 1. \qquad (43)$$

Indeed, since both k_{D-} and k_{I-} are $< k_0$, then $k_{T-} \geq k_0$. In other words, if all but one dissociation constants are smaller than the observed combination of the constants, then the remaining constant must be larger or at least the same as the observed one. For the case in which hydrolyzed subunits are prevalent on the pointed end (as it is widely assumed), this leads to the surprising conclusion that k_{T-} must be significantly larger than k_{0-}. Indeed, our analytical solution provides $k_{T-} = 0.88\ s^{-1}$, two times larger than k_{0-}, with the corresponding value, $A_{cT} = 1.57\ \mu M$, which is ~45 times higher than the value of 0.035 μM obtained for the barbed end. Note also that the case in which $k_{T-} > k_{D-}$ corresponds to case B described above in which ATP hydrolysis should promote the polymerized state since it slows down the dissociation of actin subunits. There is no such problem on the barbed end since $k_{D-} > k_{0-}$ for this end. When pointed-end rate constants are allowed to vary from prior published values to $k_{0+} = 0.2\ s^{-1} \times \mu M^{-1}$ and $k_{0-} = 0.16\ s^{-1}$ ($< k_{D-}$) (both reduced by a factor of 2.8 with the same experimental value for A_{cp} as discussed earlier), we obtain $k_{T-} = 0.007\ s^{-1}$ and satisfy all constraints. In this case the ratio $e_0 = k_{T-}/k_{D-} < 1$ is inverted, and the situation on the pointed end corresponds to case A in which ATP hydrolysis works toward depolymerization, compatible with prevailing assumptions.

One plausible explanation for the above general problem has been given by Fujiwara et al. (35), who suggested that at the pointed end, the value k_{T+} may depend on the nucleotide identity of the terminal subunit, and that the value of k_{T+} is larger when the pointed end is bound to ATP than when it is bound to ADP. For these assumptions, the equations derived in Appendix 1 are no longer valid, although the constraint described by Eq. 6 must hold. Note however that if k_{T+} strongly depends on the pointed-end nucleotide identity, the elongation rate should strongly depend on ATP-G-actin concentration until the pointed end is saturated with ATP-bound subunits at high G-actin concentrations (see section ''Experiments that can test for the presence of the suggested mechanisms''). By similar reasoning, the value of k_{T+} may also depend on concentration of inorganic phosphate. The dependence of k_{T+} for the pointed end on ATP-G-actin concentration or concentration of phosphate has not so far been observed experimentally (32,35,38), perhaps due to the low accuracy of experimental data for the pointed end. Overall, the explanation for this problem remains unsolved.

Energy difference between two actin polymerization pathways

As we mentioned above, the energy square for each pure form must be balanced, although an ''apparent'' energy square that relates apparent constants and does not distinguish between different nucleotide compositions of species is allowed to be misbalanced (Fig. 1). As mentioned above, according to experimental data from different groups, parameter Φ (Fig. 1), which characterizes the misbalance of the apparent energy square, varies between 1 and 33 (2,7,14). It is important though to establish a precise definition for this parameter. As illustrated by Fig. 1, in the presence of profilin, there are two possible pathways for actin filament elongation: the direct pathway (pathway *g* shown with a *gray arrow*) and the profilin-related pathway (pathway *pg* shown with three *purple arrows*). In the absence of profilin, there is only one

pathway g_0 (which is the pathway g in the absence of profilin although on closer scrutiny, as we now explain, it must actually be defined as a separate pathway). According to Kinosian (2) and Pantaloni and Carlier (7), the ratio of the equilibrium constants for the two elongation pathways (misbalance of the apparent energy square) is defined as

$$\Phi = [(k_-/k_+) \times K_{db}]/[(k'_-/k'_+) \times K_d], \qquad (44)$$

where k_+ and k_- are the apparent elongation and dissociation constants corresponding to the pathway g, and all other constants in Eq. 44 are related to the pathway pg. Appendix 3 provides and explains the definition of the parameter Φ, characterizing an apparent energy square (see Fig. 1) and apparent kinetic and equilibrium constants that are involved in the definition. Appendix 3 also provides equations for the standard free energy changes ($\Delta G'^0$) corresponding to actin polymerization reactions in the presence and absence of profilin. It is important to note that parameter Φ depends, in general, on profilin concentration.

Moreover, the pathway g for filament elongation in the presence of profilin is not energetically equivalent to the pathway g_0 for the filament elongation in the absence of profilin. As discussed above, the value of k_- depends on the filament nucleotide profile, which in turn, depends on the profilin concentration. Thus, there are three pathways that may be compared for the energy difference: pg, g, and g_0, each with the corresponding standard free energy change: $\Delta G'^0_{pg}$, $\Delta G'^0_g$, $\Delta G'^0_{g0}$. Therefore, at least two different definitions for the parameter Φ are possible: parameter $\Phi_{pg\text{-}g}$ related to the energy difference between the polymerization pathways pg and g ($\Delta G'^0_{pg} - \Delta G'^0_g$) and thus comparing the two pathways at the same profilin concentration (same conditions). In contrast, parameter $\Phi_{pg\text{-}g0}$ related to the energy difference between polymerization pathways pg and g_0 ($\Delta G'^0_{pg} - \Delta G'^0_{g0}$) compares one pathway at a certain profilin concentration and another pathway at zero profilin. Since the energy difference between the pathways g and g_0 (or rather dependence of the standard free energy change for the pathway g on profilin concentration) was not recognized by earlier investigators, all prior experimental evaluations for the parameter Φ actually evaluate the difference between the pathways g_0 and pg, and therefore refer to $\Phi_{pg\text{-}g0}$ as Φ (2,7,14). Fig. 8 *C* shows the differences $\Delta G'^0_{pg} - \Delta G'^0_{g0}$, $\Delta G'^0_g - \Delta G'^0_{g0}$, and $\Delta G'^0_{pg} - \Delta G'^0_g$ as functions of profilin concentration for the parameter sets *a–d* described above. In addition, panel *D* shows the difference in the standard free energy change for the combined polymerization through both pathways pg and g and the pathway g_0 $\Delta G'^0_{(pg+g)} - \Delta G'^0_{g0} = -RT \ln(A_{c0}/A_c)$.

Interestingly, in the absence of mechanism IVb, i.e., when the values of r_{n+}/K_{dn} are equal for all forms, the pathways pg and g are energetically equivalent and $\Phi_{pg\text{-}g} = 1$ for all profilin concentrations (see Appendix 3). Parameter set *a*, with only slight differences in r_{n+}/K_{dn}, corresponds approximately to this case (compare the two *black curves* of Fig. 8 *C*). The value of A_c for this set is lower in the presence of profilin due to the difference in polymerization energy between the pathways g (or pg) and g_0. One can see from Figs. 8 and 9 that the parameter set *a* is the only set for which $\Delta G'^0_g - \Delta G'^0_{g0}$ is negative since this is the only case in which profilin clearly drives the nucleotide profile toward ATP-actin, and therefore promotes polymerization through the pathway g as well as through the pathway pg. Even though the parameter sets *b*, *c*, and *d* look more favorable for the profilin pathway pg compared to the g_0 pathway, the combined polymerization through the pathways pg and g still may lead to the value of $A_c > A_{c0}$ at relatively low profilin concentrations for the set *d*. This is because the pathway g is heavily utilized at these concentrations and is energetically unfavorable relative to the g_0 pathway for the sets *b*, *c*, and *d*.

Indirect coupling of the ATP hydrolysis energy to the energy of actin polymerization

Our analysis reveals that in the absence of profilin, chemical energy of ATP hydrolysis is coupled to the chemical energy of actin polymerization through the process of monomer exchange diffusion in filamentous actin. Since exchange diffusion is a fluctuation-based process, the energy coupling is indirect. In our model, there is no direct time correlation between the events of hydrolysis and polymerization. Therefore, there is no direct energy transition to polymerization energy upon events of hydrolysis or dissociation or binding of inorganic phosphate. Part of the hydrolysis or phosphate release energy may be saved as conformation energy, resulting in allosteric changes in filamentous actin (44), and the rest of the energy likely dissipates as heat. In the absence of profilin, hydrolysis and, especially, phosphate release promote the release of actin subunits from the barbed end. Exchange diffusion, utilizing the supply of free ATP in solution and thermal energy, replaces the released hydrolyzed subunits with fresh ATP-bound subunits, the highest-energy component of the actin subunits pool, creating an energy reservoir that can be utilized by profilin. Note that the supply of energy for actin polymerization comes at the step of monomeric actin nucleotide exchange, rather than at the step of hydrolysis.

Thus, in the absence of profilin, the energy of ATP hydrolysis by polymeric actin is already indirectly coupled to the energy of actin polymerization through the process of exchange diffusion. Profilin, by enhancing exchange diffusion, modifies this coupling, increasing the ATP content (and free energy) of actin polymer and thereby promoting the transition of the stored energy of monomeric actin into actin polymerization. Allosteric changes in actin due to polymerization, profilin, and/or nucleotide binding, ATP hydrolysis, and phosphate release may play an important role in the modification mechanism (44,45). Differential binding of profilin to different monomeric forms of actin may provide additional energy by the creation of an alternative pathway for the utilization of the energy of ATP hydrolysis, thus providing the source of the energy-driving mechanism IVb.

(See Fig. 8 *D* and Appendix 3). In this regard, mechanism IVb is potentially a more powerful mechanism than mechanism V. At the limit of very high profilin concentration, exchange diffusion in mechanism V could maximally convert F-actin from a mixture of forms to one exclusively composed of ATP-F-actin, with the thermodynamic consequence that A_{cb} will not decrease to less than A_{cT}. Mechanism IVb does not have this thermodynamic limitation. Note although that even with active mechanism IVb, ATP hydrolysis also does not provide a direct energy supply but rather acts as a brake in the depolymerization process, allowing utilization of the thermal energy of the subunit exchange.

Note a similarity of this case to other models that are based on the same general principle of indirect energy coupling, for example, to the Brownian ratchet models of molecular motors (45–64). In ordinary motors, energy input causes motion. In the Brownian ratchet models of molecular motors, an energy input restrains motion. Note also that in the F1-ATP synthase motor (in the mode when it operates as an ion pump), the actual torque-generating step takes place during the binding of ATP to the catalytic site; the role of the hydrolysis step is to release the hydrolysis products, allowing the cycle to repeat (65). Note, though, that our hypothesis is related to the Brownian ratchet theory only through the fact that both are based on the same general physical principle for indirect coupling of energy (see for review Ait-Haddou and Herzog (47)) and that our model does not calculate the displacement or force production. The Brownian ratchet theory employs the idea for indirect coupling of the chemical energy of actin polymerization to mechanical energy, and our model provides an explanation of how the chemical energy of ATP hydrolysis could be coupled to the chemical energy of actin polymerization and how profilin could modulate this coupling. An increasing amount of theoretical and experimental research suggests that indirect energy coupling underlies various biologic processes (45–64). Indirect energy coupling represents a fundamental change in the paradigm of energy utilization in biological systems. It introduces a time delay with indirect transfer of chemical energy. The advantage of such a mechanism is the removal of certain time constraints that limited the accuracy of models of biological systems based on the prior paradigm.

To understand the profilin mechanism in detail, one needs first to clearly understand the role of ATP hydrolysis and phosphate release in actin polymerization at various conditions including nonsteady-state conditions. The detailed mechanism of energy coupling as well as a full explanation of the role of ATP hydrolysis in actin polymerization needs further investigation.

Experiments that can test for the presence of the suggested mechanisms

Note that at nonsteady-state conditions, $A_{c0} = k_{0-}/k_{0+}$ is, in general, a function of G-actin concentration due to the dependence of k_{0-} on the nucleotide identity of the filament end. The experimentally obtained dependence of A_c on G-actin concentration in the absence of profilin could provide evidence supporting the importance of mechanism V. Indeed, note that mechanism V requires low A_{cT}. At high concentrations of monomeric actin, filament ends should become predominately ATP bound, and polymerization and depolymerization occur mainly through ATP-bound actin. Then the value of A_{cT} can be obtained from the x intercept of the dependence of the polymerization rate on G obtained at high concentrations of monomeric actin. This value can be compared with the value of $A_c^{(Sat)}$ obtained at saturation with profilin at steady-state conditions in the experiment as shown in Fig. 6 (*inset 2*). The result $A_c^{(Sat)} = A_{cT}$ supports the existence of mechanism V only, and the result $A_c^{(Sat)}/A_{cT} < 1$ would support the conclusion that mechanism IVb is important. For the pointed end, the dependence of the polymerization rate on G could provide information regarding the dependence of the k_{T+} on the nucleotide identity of the end (see discussion in the section ''Consequences of thermodynamic constraints on parameters for the pointed end'') as well as A_{cT}.

Implications for possible in vivo effects of profilin

In vivo, filaments are arrayed into complex networks (lamellipodia or filipodia) combining thousands of filaments with their barbed ends located at or near the membrane. The stochastic process of indirect coupling between ATP hydrolysis and actin polymerization is averaged over a large population of independent barbed ends. With a large number of barbed ends, the acceleration of monomeric nucleotide exchange may become important and then mechanism II should also come into play under these conditions. Profilin accelerates both monomeric nucleotide exchange (mechanism II) and polymeric subunit exchange (mechanism V). Close to the membrane, where actin filaments undergo active polymerization, barbed ends may become predominately ATP bound, if mechanism V prevails, or ADP-bound, if mechanism IVb in combination with acceleration of hydrolysis is prevalent (see Fig. 9). Thus under these conditions exchange diffusion and/or profilin help to synchronize the barbed ends' nucleotide states and, therefore, the rate of polymerization. At depolymerization conditions, synchronization should be favored by profilin, ATP hydrolysis, and mechanical interactions with the membrane. If diffusion of G-actin to the local area at or near the membrane is time limiting, mechanism I will not be active, A_c may be close to A_{cb}, and analysis limited to a single end is applicable. On the other hand, if diffusion is relatively fast, mechanism I may become active.

In a local area behind the active polymerization zone, the presence of severing proteins (especially those like cofilin, which sever actin filaments but do not cap the barbed end), the ADP and ADP-Pi core of actin filaments may become

exposed and then A_{cb}^{local} would increase. This may lead to a switch to the fast barbed-end depolymerization in this area promoted by profilin. Indeed, even though profilin decreases A_{cb} and promotes polymerization at the barbed end when concentration of free monomeric actin $G > A_{cb}$, at conditions when $G < A_{cb}^{local}$, profilin will promote enrichment of the end with hydrolyzed forms and accelerate depolymerization, simultaneously increasing A_{cb}^{local}. Therefore, profilin could act in this area as a factor that promotes rapid depolymerization. The rate of profilin-accelerated depolymerization could be up to $1000 \times k_{D-}$ (see Eq. 33). Thus, acting on barbed ends in tandem with severing proteins behind the area of active polymerization in lamellipodia or filopodia, profilin could help to provide fresh ATP-bound monomers much faster than could the pointed ends for active polymerization closer to the membrane.

CONCLUSIONS

Our study demonstrates that

1. The effect of profilin on A_c can be explained in a manner consistent with thermodynamic constraints.
2. The existence of the pointed end, and therefore treadmilling, is not necessary for profilin to decrease A_c.
3. The acceleration of ADP-ATP exchange of G-actin (mechanism II) is unlikely to be a significant mechanism related to the effect of profilin on A_c.
4. The suggestion that the differential binding of nucleotides to monomeric actin and to the profilin-actin complex results in reduced A_c (mechanism III) (2) violates thermodynamic constraints.
5. The A_c is defined mainly by two ratios: the ratio of the rates of depolymerization of ATP- and ADP- (or ADP-Pi-) bound filament ends (depolymerization rates ratio) and the ratio of the rate of exchange diffusion to the rate of simple cycling of ATP-bound subunits between monomeric and polymeric forms (exchange diffusion ratio).
6. The mechanism for the effect of profilin on actin polymerization may be based on a general principle of indirect energy coupling. Such coupling may occur through effects on the depolymerization rates ratio (mechanism IVb) and/or the exchange diffusion ratio (mechanism V).
7. In the absence of profilin, the ratio k_{T-}/k_{Y-} (the depolymerization rates ratio in this case) mainly defines the role of ATP hydrolysis in actin polymerization at the particular filament end (where index Y stands for either I or D; $Y = D$ is applicable for low (100 μM or less); and $Y = I$ for high (50–100 mM) inorganic phosphate concentrations). Hydrolysis promotes either a polymerized or a depolymerized state depending on this ratio.
8. Profilin can modulate the role of ATP hydrolysis by changing the depolymerization rates ratio and may even invert the role of hydrolysis and turn it from a factor working against polymerization to a factor that promotes polymerization (mechanism IVb).
9. Profilin can promote actin polymerization through acceleration of the monomeric subunit exchange (mechanism V), for which, paradoxically, a faster rate of actin depolymerization promotes net polymerization.
10. Conventional calculations of energy imbalance, Φ, have neglected differences between the pathways for the addition of a free actin subunit that occurs in the presence of profilin compared to the absence of profilin.
11. Profilin can lower A_c even when the two pathways of actin elongation in the presence of profilin (as free actin or profilin-actin complex) are energetically equivalent. In this case, the existence of the pathway for the addition of profilin-actin can drive the filament nucleotide profile toward ATP-F-actin, making both pathways more energetically favorable than the single pathway available in the absence of profilin.

APPENDIX 1: EQUATIONS AND DERIVATION OF ANALYTICAL RESULTS

Part 1: equations

Variables are defined in Table 1. Chemical reactions, parameter definitions, and thermodynamic constraints are shown in Fig. 3. According to the considered chemical reactions, assumptions, idealizations, and constraints, the following equations can be written.

Constraints

Actin-profilin polymerization energy square (detailed balance) for each nucleotide form (see Figs. 1 and 3):

$$\Phi_n = ((k_{n-}/k_{n+}) \times K_{dbn})/((k'_{n-}/k'_{n+}) \times K_{dn}) = 1. \quad (A1)$$

Energy square (detailed balance) for the addition of phosphate (Pi) and profilin to the filament end with ADP- and ADP-Pi-carrying subunits (see Fig. 3):

$$(K_{dPi} \times K_{dbI})/(K'_{dPi} \times K_{dbD}) = 1. \quad (A2)$$

The other thermodynamic constrains shown on Fig. 3 and the constraints described by Eq. 6 were not used for the derivation of equations for A_c and the actin filament nucleotide profile. Although we used them to calculate certain parameters (see Table 2) and fractions, r_n of the particular nucleotide form in the total free monomeric actin pool (see Table 1 and Eqs. A82–A85).

Steady-state equations

The concentration of the complex of profilin with monomeric actin of a particular nucleotide type n is defined by the affinity of profilin to this form of G-actin:

$$[Pn]/n = P/K_{dn}. \quad (A3)$$

It is widely accepted that profilin dissociates from the filament end at a high rate (2,9,14,24). This implies fast equilibration of free profilin with the filament ends. Thus the percentage of the ends containing a particular nucleotide in the terminal subunit capped by profilin is defined by the affinity of profilin to that particular form of end:

$$g_{\mathrm{Pn}(1)} = g_{\mathrm{n}(1)} \times P/K_{\mathrm{dbn}}. \quad \text{(A4)}$$

There is no net polymerization for each filament. Subunit exchange E is defined by steady-state polymerization and depolymerization:

$$E = k_{\mathrm{ON}} = k_{\mathrm{OFF}} \quad \text{(A5)}$$

$$k_{\mathrm{ON}} = g_{\mathrm{f}} \times \sum(k_{\mathrm{n}+} \times n + k'_{\mathrm{n}+} \times [Pn]) \quad \text{(A6)}$$

$$k_{\mathrm{OFF}} = \sum(g_{\mathrm{n}(1)} \times k_{\mathrm{n}-} + g_{\mathrm{Pn}(1)} \times k'_{\mathrm{n}-}). \quad \text{(A7)}$$

There is no net formation of filamentous subunits of any type. Note that as defined in Table 1, i is the distance (in the number of subunits) from the filament end so that $i = 1$ always corresponds to the end subunit. Then at polymerization or depolymerization events, i changes for the particular physical subunit.

For $i \geq 3$,

$$d(g_{\mathrm{A(i)}})/dt = 0 = k_{\mathrm{ON}} \times (g_{\mathrm{A(i-1)}} - g_{\mathrm{A(i)}}) + k_{\mathrm{OFF}} \times (g_{\mathrm{A(i+1)}} - g_{\mathrm{A(i)}}) \quad \text{(A8)}$$

$$d(g_{\mathrm{T(i)}})/dt = 0 = k_{\mathrm{ON}} \times (g_{\mathrm{T(i-1)}} - g_{\mathrm{T(i)}}) + k_{\mathrm{OFF}} \times (g_{\mathrm{T(i+1)}} - g_{\mathrm{T(i)}}) - k_{\mathrm{H}} \times g_{\mathrm{T(i)}} \quad \text{(A9)}$$

$$d(g_{\mathrm{I(i)}})/dt = 0 = k_{\mathrm{ON}} \times (g_{\mathrm{I(i-1)}} - g_{\mathrm{I(i)}}) + k_{\mathrm{OFF}} \times (g_{\mathrm{I(i+1)}} - g_{\mathrm{I(i)}}) + k_{\mathrm{H}} \times g_{\mathrm{T(i)}} - k_{\mathrm{Pi}-} \times g_{\mathrm{I(i)}} + k_{\mathrm{Pi}+} \times [\mathrm{Pi}] \times g_{\mathrm{D(i)}} \quad \text{(A10)}$$

$$g_{\mathrm{D(i)}} = 1 - g_{\mathrm{A(i)}} - g_{\mathrm{T(i)}} - g_{\mathrm{I(i)}}. \quad \text{(A11)}$$

For $i = 2$,

$$d(g_{\mathrm{A(2)}})/dt = 0 = k_{\mathrm{ON}} \times (g_{\mathrm{A(1)}}/g_{\mathrm{f}} - g_{\mathrm{A(2)}}) + k_{\mathrm{OFF}} \times (g_{\mathrm{A(3)}} - g_{\mathrm{A(2)}}) \quad \text{(A12)}$$

$$d(g_{\mathrm{T(2)}})/dt = 0 = k_{\mathrm{ON}} \times (g_{\mathrm{T(1)}}/g_{\mathrm{f}} - g_{\mathrm{T(2)}}) + k_{\mathrm{OFF}} \times (g_{\mathrm{T(3)}} - g_{\mathrm{T(2)}}) - k_{\mathrm{H}} \times g_{\mathrm{T(2)}} \quad \text{(A13)}$$

$$d(g_{\mathrm{I(2)}})/dt = 0 = k_{\mathrm{ON}} \times (g_{\mathrm{I(1)}}/g_{\mathrm{f}} - g_{\mathrm{I(2)}}) + k_{\mathrm{OFF}} \times (g_{\mathrm{I(3)}} - g_{\mathrm{I(2)}}) + k_{\mathrm{H}} \times g_{\mathrm{T(2)}} - k_{\mathrm{Pi}-} \times g_{\mathrm{I(2)}} + k_{\mathrm{Pi}+} \times [\mathrm{Pi}] \times g_{\mathrm{D(2)}} \quad \text{(A14)}$$

$$g_{\mathrm{D(2)}} = 1 - g_{\mathrm{A(2)}} - g_{\mathrm{T(2)}} - g_{\mathrm{I(2)}}. \quad \text{(A15)}$$

For filament ends ($i = 1$),

$$d(g_{\mathrm{A(1)}} + g_{\mathrm{PA(1)}})/dt = 0 = k_{\mathrm{A}+} \times A \times (g_{\mathrm{f}} - g_{\mathrm{A(1)}}) - (k_{\mathrm{ON}} - k_{\mathrm{A}+} \times A \times g_{\mathrm{f}}) \times (g_{\mathrm{A(1)}}/g_{\mathrm{f}}) + (k_{\mathrm{OFF}} - k_{\mathrm{A}-} \times g_{\mathrm{A(1)}}) \times g_{\mathrm{A(2)}} - k_{\mathrm{A}-} \times g_{\mathrm{A(1)}} \times (1 - g_{\mathrm{A(2)}}) + k'_{\mathrm{A}+} \times [PA] \times g_{\mathrm{f}} - k'_{\mathrm{A}-} \times g_{\mathrm{PA(1)}} \quad \text{(A16)}$$

$$d(g_{\mathrm{T(1)}} + g_{\mathrm{PT(1)}})/dt = 0 = k_{\mathrm{T}+} \times T \times (g_{\mathrm{f}} - g_{\mathrm{T(1)}}) - (k_{\mathrm{ON}} - k_{\mathrm{T}+} \times T \times g_{\mathrm{f}}) \times (g_{\mathrm{T(1)}}/g_{\mathrm{f}}) + (k_{\mathrm{OFF}} - k_{\mathrm{T}-} \times g_{\mathrm{T(1)}}) \times g_{\mathrm{T(2)}} - k_{\mathrm{T}-} \times g_{\mathrm{T(1)}} \times (1 - g_{\mathrm{T(2)}}) - k_{\mathrm{He}} \times g_{\mathrm{T(1)}} + k'_{\mathrm{T}+} \times [PT] \times g_{\mathrm{f}} - k'_{\mathrm{T}-} \times g_{\mathrm{PT(1)}} - k'_{\mathrm{He}} \times g_{\mathrm{PT(1)}} \quad \text{(A17)}$$

$$d(g_{\mathrm{I(1)}} + g_{\mathrm{PI(1)}})/dt = 0 = k_{\mathrm{I}+} \times I \times (g_{\mathrm{f}} - g_{\mathrm{I(1)}}) - (k_{\mathrm{ON}} - g_{\mathrm{f}} \times k_{\mathrm{I}+} \times I) \times (g_{\mathrm{I(1)}}/g_{\mathrm{f}}) + (k_{\mathrm{OFF}} - g_{\mathrm{I(1)}} \times k_{\mathrm{I}-}) \times g_{\mathrm{I(2)}} - k_{\mathrm{I}-} \times g_{\mathrm{I(1)}} \times (1 - g_{\mathrm{I(2)}}) + k_{\mathrm{He}} \times g_{\mathrm{T(1)}} + k_{\mathrm{Pie}+} \times [\mathrm{Pi}] \times g_{\mathrm{D(1)}} - k_{\mathrm{Pie}-} \times g_{\mathrm{I(1)}} + k'_{\mathrm{I}+} \times [\mathrm{Pi}] \times g_{\mathrm{f}} - k'_{\mathrm{I}-} \times g_{\mathrm{PI(1)}} + k'_{\mathrm{He}} \times g_{\mathrm{PT(1)}} + k'_{\mathrm{Pie}+} \times [\mathrm{Pi}] \times g_{\mathrm{PD(1)}} - k'_{\mathrm{Pie}-} \times g_{\mathrm{PI(1)}} \quad \text{(A18)}$$

$$\sum(g_{\mathrm{n}(1)} + g_{\mathrm{Pn}(1)}) = 1. \quad \text{(A19)}$$

Part 2: derivation of expressions for A_c and for the filament nucleotide profile

Combining Eqs. A3–A7 gives

$$E = g_{\mathrm{f}} \times \sum k_{\mathrm{n}+} \times n \times [1 + (k'_{\mathrm{n}+}/k_{\mathrm{n}+}) \times P/K_{\mathrm{dn}}] = \sum g_{\mathrm{n}(1)} \times k_{\mathrm{n}-} \times [1 + (k'_{\mathrm{n}-}/k_{\mathrm{n}-}) \times P/K_{\mathrm{dbn}}]. \quad \text{(A20)}$$

Combining Eqs. A1 and A20 gives

$$E = g_{\mathrm{f}} \times A_c \times \sum(r_{\mathrm{n}} \times S_{\mathrm{n}} \times k_{\mathrm{n}+}) = \sum(g_{\mathrm{n}(1)} \times S_{\mathrm{n}} \times k_{\mathrm{n}-}), \quad \text{(A21)}$$

where

$$S_{\mathrm{n}} = 1 + r_{\mathrm{n}+} P/K_{\mathrm{dn}}. \quad \text{(A22)}$$

Combining Eqs. A5 and A8–A11 gives

For $i \geq 3$,

$$E \times g_{\mathrm{A(i-1)}} - 2E \times g_{\mathrm{A(i)}} + E \times g_{\mathrm{A(i+1)}} = 0 \quad \text{(A23)}$$

$$E \times g_{\mathrm{T(i-1)}} - (2E + k_{\mathrm{H}}) \times g_{\mathrm{T(i)}} + E \times g_{\mathrm{T(i+1)}} = 0 \quad \text{(A24)}$$

$$E \times g_{\mathrm{I(i-1)}} - (2E + k_1 + k_2) \times g_{\mathrm{I(i)}} + E \times g_{\mathrm{I(i+1)}} + (k_{\mathrm{H}} - k_1) \times g_{\mathrm{T(i)}} - k_1 \times g_{\mathrm{A(i)}} + k_1 = 0 \quad \text{(A25)}$$

$$g_{\mathrm{D(i)}} = 1 - g_{\mathrm{A(i)}} - g_{\mathrm{T(i)}} - g_{\mathrm{I(i)}} \quad \text{(A26)}$$

where

$$k_1 = k_{\mathrm{Pi}+} \times [\mathrm{Pi}] \text{ and } k_2 = k_{\mathrm{Pi}-}. \quad \text{(A27)}$$

Combining Eqs. A5 and A12–A15 gives

For $i = 2$,

$$E \times g_{\mathrm{A(1)}}/g_{\mathrm{f}} - 2E \times g_{\mathrm{A(2)}} + E \times g_{\mathrm{A(3)}} = 0 \quad \text{(A28)}$$

$$E \times g_{\mathrm{T(1)}}/g_{\mathrm{f}} - (2E + k_{\mathrm{H}}) \times g_{\mathrm{T(2)}} + E \times g_{\mathrm{T(3)}} = 0 \quad \text{(A29)}$$

$$E \times g_{\mathrm{I(1)}}/g_{\mathrm{f}} - (2E + k_1 + k_2) \times g_{\mathrm{I(2)}} + E \times g_{\mathrm{I(3)}} + (k_{\mathrm{H}} - k_1) \times g_{\mathrm{T(2)}} - k_1 \times g_{\mathrm{A(2)}} + k_1 = 0 \quad \text{(A30)}$$

$$g_{\mathrm{D(2)}} = 1 - g_{\mathrm{A(2)}} - g_{\mathrm{T(2)}} - g_{\mathrm{I(2)}}. \quad \text{(A31)}$$

Equations similar to Eqs. A23–A31 are solved in Bindschadler et al. (24). In our case the solution is

For all $i \geq 2$,

$$g_{A(i)} = C_A \tag{A32}$$

$$g_{T(i)} = C_T \times (\lambda_-)^i + C'_T \times (\lambda_+)^i \tag{A33}$$

$$g_{I(i)} = C_1 \times (\delta_-)^i + C_2 \times (\lambda_-)^i + C_3 + C'_1 \times (\delta_+)^i + C'_2 \times (\lambda_+)^i, \tag{A34}$$

where C_A, C_T, C_1, C_2, C_3, C'_T, C'_1, and C'_2 are arbitrary constants to be determined from boundary conditions, and

$$\lambda_\pm = (1 + k_H/2E) \pm (k_H/2E) \times (1 + 4E/k_H)^{1/2} \tag{A35}$$

$$\delta_\pm = (1 + (k_1 + k_2)/2E) \pm ((k_1 + k_2)/2E) \times (1 + 4E/(k_1 + k_2))^{1/2}. \tag{A36}$$

Note that since always $\lambda_+ > 1$, $\delta_+ > 1$, $0 < \lambda_- < 1$, $0 < \delta_- < 1$, and the number of subunits i in the filament is not limited in our model (assumption 5), and there must be $g_{n(i)} \leq 1$ for all subunits including the filament core where i is very large, the coefficients C'_T, C'_1, C'_2 must be equal to zero.

Substituting Eqs. A37–A40 into Eqs. A28–A31 gives

$$g_{A(1)} = g_f \times C_A \tag{A50}$$

$$g_{T(1)} = g_f \times C_T \times \lambda \tag{A51}$$

$$g_{I(1)} = g_f \times (C_1 \times \delta + C_2 \times \lambda + C_3) \tag{A52}$$

$$g_{D(1)} = g_f \times (1 - C_A - C_T \times \lambda - C_1 \times \delta - C_2 \times \lambda - C_3), \tag{A53}$$

where

$$g_f = [q_D + C_A \times (q_A - q_D) + C_T \times \lambda \times (q_T - q_D) + (C_1 \times \delta + C_2 \times \lambda + C_3) \times (q_I - q_D)]^{-1}. \tag{A54}$$

Then, combining Eqs. A1–A5, A16–A18, A21, A27, and A37–A53 leads to

$$C_T \times \lambda = ([T]/A_{cT}) \times [1 + \alpha \times k_H/(S_T \times k_{T-})]^{-1} \tag{A55}$$

and

$$C_1 \times \delta + C_2 \times \lambda + C_3 = \{[I]/A_{cI} + (C_T \times \lambda \times \varphi/(S_I \times k_{I-})) \times [k_H \times (\alpha + \gamma) - \beta \times (k_1 + k_2)] + (1 - C_A) \times \beta \times k_1/(S_I \times k_{I-})\}(1 + \beta \times (k_1 + k_2)/(S_I \times k_{I-}))^{-1}, \tag{A56}$$

Then, for $i \geq 2$, one obtains the filament nucleotide profile equations

$$g_{A(i)} = C_A \tag{A37}$$

$$g_{T(i)} = C_T \times \lambda^i \tag{A38}$$

$$g_{I(i)} = C_1 \times \delta^i + C_2 \times \lambda^i + C_3 \tag{A39}$$

$$g_{D(i)} = 1 - g_{A(i)} - g_{T(i)} - g_{I(i)}, \tag{A40}$$

where

$$\lambda = 1 - (k_H/2E) \times ((1 + 4E/k_H)^{1/2} - 1) \tag{A41}$$

$$\delta = 1 - ((k_1 + k_2)/2E) \times ((1 + 4E/(k_1 + k_2))^{1/2} - 1) \tag{A42}$$

$$C_2 = -C_T \times \varphi \tag{A43}$$

$$C_3 = (1 - C_A) \times \psi \tag{A44}$$

$$\psi = k_1/(k_1 + k_2) \tag{A45}$$

$$\varphi = (k_H - k_1)/(k_H - (k_1 + k_2)) = (1 + k_2/(k_H - (k_1 + k_2)). \tag{A46}$$

For $i = 1$,

by combining Eqs. A4 and A19 one obtains

$$\sum g_{n(1)} \times q_n = 1, \tag{A47}$$

where

$$q_n = 1 + P/K_{dbn}, \tag{A48}$$

and

$$g_{D(1)} \times q_D = 1 - (g_{A(1)} \times q_A + g_{T(1)} \times q_T + g_{I(1)} \times q_I). \tag{A49}$$

$$C_A = r_A \times A_c/A_{cA} \tag{A57}$$

$$C_T = A_c \times r_T \times A_{cT}^{-1}/(f_{T\alpha} \times \lambda) \tag{A58}$$

$$C_1 = A_c \times \{r_I \times A_{cI}^{-1} + r_A \times A_{cA}^{-1} \times \psi + r_T \times A_{cT}^{-1} \times \varphi \times [f_{I\alpha} + k_H \times \gamma/(S_I \times k_{I-})]/f_{T\alpha} - A_c^{-1} \times \psi\}/(f_{I\beta} \times \delta), \tag{A59}$$

where

$$f_{T\alpha} = 1 + \alpha \times k_H/(S_T \times k_{T-}) \tag{A60}$$

$$f_{I\alpha} = 1 + \alpha \times k_H/(S_I \times k_{I-}) \tag{A61}$$

$$f_{I\beta} = 1 + \beta \times (k_1 + k_2)/(S_I \times k_{I-}) \tag{A62}$$

$$\alpha = S_H + g_f^{-1} \times \lambda/(1 - \lambda) \tag{A63}$$

$$\beta = S_{Pi} + g_f^{-1} \times \delta/(1 - \delta) \tag{A64}$$

$$\gamma = k_2 \times (S_{Pi} - S_H)/(k_H - k_1) \tag{A65}$$

$$S_H = r_{He} \times (1 + r_H \times P/K_{dbT}) \tag{A66}$$

$$S_{Pi} = r_{Pie} \times (1 + r_{Pi} \times P/K_{dbI}), \tag{A67}$$

and to

$$A_c \times \sum r_n \times U_n^{-1} \times A_{cn}^{-1} = 1 \tag{A68}$$

where

$$U_A = 1 \tag{A69}$$

$$U_D = f_\beta/f_{I\beta} \tag{A70}$$

$$U_I = f_\beta / f_{D\beta} \tag{A71}$$

$$U_T = (f_\beta \times f_{T\alpha}) / (f_{D\beta} \times f_{I\alpha} + f_T), \tag{A72}$$

and

$$f_\beta = 1 + \beta \times [k_1/(S_D \times k_{D-}) + k_2/(S_I \times k_{I-})] \tag{A73}$$

$$f_{D\beta} = 1 + \beta \times (k_1 + k_2)/(S_D \times k_{D-}) \tag{A74}$$

$$f_T = [1 - (S_I \times k_{I-})/(S_D \times k_{D-})] \times f_{\alpha\beta} \tag{A75}$$

$$f_{\alpha\beta} = [k_2/(S_I \times k_{I-})] \times \{S_{Pi} + [(\alpha - S_H) \times k_H - (\beta - S_{Pi}) \times (k_1 + k_2)]/[k_H - (k_1 + k_2)]\}. \tag{A76}$$

Then the filament tip nucleotide identities

$$g_A = r_A \times A_c / A_{cA} \tag{A77}$$

$$g_T = r_T \times A_c \times A_{cT}^{-1} / f_{T\alpha} \tag{A78}$$

$$g_I = \{(1 - g_A) \times \beta \times k_1/(S_I \times k_{I-}) + r_I \times A_c \times A_{cI}^{-1} + g_T \times (f_{T\alpha} + f_{\alpha\beta} - f_{I\beta})\}/f_{I\beta} \tag{A79}$$

$$g_D = \{(1 - g_A) \times [1 + \beta \times k_2/(S_I \times k_{I-})] - r_I \times A_c \times A_{cI}^{-1} - g_T \times (f_{T\alpha} + f_{\alpha\beta})\}/f_{I\beta}. \tag{A80}$$

where (see Table 1)

$$g_n = g_{n(1)}/g_f. \tag{A81}$$

Part 3: derivation of parameters from experimental results

Assuming that mechanism II (see text) is not in effect, i.e., that the concentrations of monomeric actin forms are defined only by the affinities of nucleotide-free actin to ATP and ADP, and the affinity of phosphate to monomeric ADP-actin, one obtains

$$r_T = r_A \times [ATP]/K_{dATP} \tag{A82}$$

$$r_D = r_A \times [ADP]/K_{dADP} \tag{A83}$$

$$r_I = r_D \times [Pi]/K_{dGPi} = r_A \times [ADP] \times [Pi]/(K_{dADP} \times K_{dGPi}) \tag{A84}$$

$$r_A = (1 + [ADP]/K_{dADP} + [ATP]/K_{dATP} + [ADP] \times [Pi]/(K_{dADP} \times K_{dGPi}))^{-1}. \tag{A85}$$

It is possible to solve analytically the system of Eqs. A37–A85 to obtain parameters k_{T-} (or A_{cT}), K_{dbT}, and r_H if all other parameters are known and the values of A_c and K_{db} are defined experimentally in the absence and presence of a certain concentration of profilin. Indeed, A_c and K_{db} can be obtained experimentally, and g_f can be calculated as $g_f = (1 + P/K_{db})^{-1}$. Coefficients U_A, U_D, and U_I do not depend on k_{T-} and can be calculated using Eqs. A69–A71. Then, one obtains from Eq. A68

$$r_T \times U_T^{-1} \times A_{cT}^{-1} = (A_c^{-1} - r_A \times U_A^{-1} \times A_{cA}^{-1} - r_D \times U_D^{-1} \times A_{cD}^{-1} - r_I \times U_I^{-1} \times A_{cI}^{-1}) \tag{A86}$$

or

$$B = U_T \times k_{T-} = r_T \times k_{T+} \times (A_c^{-1} - r_A \times U_A^{-1} \times A_{cA}^{-1} - r_D \times U_D^{-1} \times A_{cD}^{-1} - r_I \times U_I^{-1} \times A_{cI}^{-1})^{-1}. \tag{A87}$$

From Eqs. A72 and A60, one obtains

$$U_T = [1 + \alpha \times k_H/(S_T \times k_{T-})] \times L \tag{A88}$$

where

$$L = f_\beta / (f_{D\beta} \times f_{I\alpha} + f_T). \tag{A89}$$

In the absence of profilin $g_f = S_T = 1$ and $S_H = r_{He}$, then α_0 (index "0" refers to the absence of profilin) can be calculated using Eqs. A21, A41, and A63. L and B do not depend on k_{T-} and can be calculated using Eqs. A61, A73–A75, A87, and A89. Then, combining Eqs. A87 and A88,

$$B_0 = U_{T0} \times k_{T-} = (k_{T-} + \alpha_0 \times k_H) \times L_0, \tag{A90}$$

and

$$k_{T-} = B_0/L_0 - \alpha_0 \times k_H. \tag{A91}$$

In the presence of profilin one obtains from Eqs. A60–A61, A63, and A72,

$$U_T = f_\beta \times [1 + \alpha \times k_H/(S_T \times k_{T-})]/\{[1 + \alpha \times k_H/(S_I \times k_{I-})] \times f_{D\beta} + f_T\} \tag{A92}$$

$$\alpha - S_H = g_f^{-1} \times \lambda/(1 - \lambda). \tag{A93}$$

Then, by combining Eqs. A87 and A92

$$k_{T-} \times f_\beta \times [1 + \alpha \times k_H/(S_T \times k_{T-})]/\{[1 + \alpha \times k_H/(S_I \times k_{I-})] \times f_{D\beta} + f_T\} = B \tag{A94}$$

and

$$\alpha = [f_\beta \times k_{T-} - B(f_T + f_{D\beta})]/\{k_H \times [B \times f_{D\beta}/(S_I \times k_{I-}) - f_\beta/S_T]\}. \tag{A95}$$

Then from Eqs. A48 and A54, one obtains

$$q_T = \{g_f^{-1} - [q_D + C_A \times (q_A - q_D) + (C_1 \times \delta + C_2 \times \lambda + C_3) \times (q_I - q_D)]\}/C_T \times \lambda + q_D \tag{A96}$$

or

$$(K_{dbT})^{-1} = (K_{dbD})^{-1} + \{[(K_{db})^{-1} - (K_{dbD})^{-1}] - C_A \times [(K_{dbA})^{-1} - (K_{dbD})^{-1}] - (C_1 \times \delta + C_2 \times \lambda + C_3) \times [(K_{dbI})^{-1} - (K_{dbD})^{-1}]\}/C_T \times \lambda, \tag{A97}$$

where coefficients C_k can be found from Eqs. A43–A46 and A57–A59. Parameter r_H can be found from Eqs. A63 and A66:

$$S_H = \alpha - g_f^{-1} \times \lambda/(1 - \lambda) \tag{A98}$$

$$r_H = K_{dbT} \times (S_H/r_{He} - 1)/P. \tag{A99}$$

Or, instead, one could define experimentally or set up for theoretical analysis the value of $w = K_{dbD}/K_{dbT}$ and then obtain the values of r_H, K_{dbT}, and K_{dbD}:

$$K_{dbD} = [C_T \times \lambda \times (w - 1) + (1 - C_A - C_T \times \lambda - C_1 \times \delta - C_2 \times \lambda - C_3)]/[K_{db}^{-1} - C_A \times K_{dbA}^{-1} - (C_1 \times \delta + C_2 \times \lambda + C_3) \times K_{dbI}^{-1}] \tag{A100}$$

$$K_{dbT} = K_{dbD}/w, \tag{A101}$$

and r_H is defined by Eq. A99.

APPENDIX 2: LIMITING CASES

Part 1: a hypothetical case at conditions with low Pi and excess of ATP when the rates of ATP hydrolysis and phosphate release are much higher than the rates of polymerization and depolymerization

At low phosphate concentrations, $k_2 \gg k_1$, and when

$$S_H \times k_H \gg S_n \times k_{n-}, \quad S_{Pi} \times k_2 \gg S_D \times k_{D-}, \quad S_{Pi} \times k_2 \gg S_I \times k_{I-}, \tag{B1}$$

one obtains from Eqs. A69–A72

$$U_A = 1 \tag{B2}$$

$$U_D \approx 1 \tag{B3}$$

$$U_I \approx (S_D \times k_{D-})/(S_I \times k_{I-}) \tag{B4}$$

$$U_T \approx (S_D \times k_{D-})/(S_T \times k_{T-}). \tag{B5}$$

At these conditions

$$\lambda \approx E^2/k_H^2 \ll 1, \quad \alpha \approx S_H, \quad \delta \approx E^2/k_2^2 \ll 1, \quad \beta \approx S_{Pi}, \quad \text{and} \quad E \approx S_D \times k_{D-}/q_D. \tag{B6}$$

Wegner (22) considered this case (with immediate exchange of ADP-Pi and ADP for ATP by G-actin). For this case $r_T = 1$, and $r_D = r_I = r_A = 0$. Then one obtains from Eq. A68

$$A_c = U_T \times A_{cT} = (S_D \times k_{D-})/(S_T \times k_{T+}), \tag{B7}$$

and in the absence of profilin

$$A_c = k_{D-}/k_{T+}. \tag{B8}$$

according to the result obtained in Wegner (22).

Part 2: hypothetical cases when the rate of hydrolysis is comparable to the rate of subunit exchange and either i), parameters for ADP and ADP-Pi actin forms are the same or phosphate release is very slow compared to hydrolysis, or ii), overall phosphate release is very fast compared to hydrolysis

i. When $S_D \times k_{D-} = S_I \times k_{I-}$, according to Eqs. A60–A62 and A73–A75, $f_\beta = f_{I\beta} = f_{D\beta}, f_T = 0$, and Eqs. A69–A72 reduce to

$$U_A = 1 \tag{B9}$$

$$U_D = 1 \tag{B10}$$

$$U_I = 1 \tag{B11}$$

$$U_T = f_{T\alpha}/f_{I\alpha} = [1 + \alpha \times k_H/(S_T \times k_{T-})]/[1 + \alpha \times k_H/(S_I \times k_{I-})]. \tag{B12}$$

The same result is obtained for the case when phosphate release is very slow compared to the hydrolysis and subunit exchange ($r_{Pie} \approx 1$). In this case,

$$\beta \times (k_1 + k_2)/(S_I \times k_{I-}) \ll 1, \quad \beta \times (k_1 + k_2)/(S_D \times k_{D-}) \ll 1, \quad \text{and} \quad \beta \times (k_1 + k_2) \ll \alpha \times k_H, \tag{B13}$$

and the values of U_n are defined by Eqs. B9–B12.

ii. The case when phosphate release is very fast compared to the rates of hydrolysis and subunit exchange could be realized if $r_{Pie} \gg r_{He} \times k_H/(k_1 + k_2)$, as suggested in Fujiwara et al. (35). This case corresponds to the set of parameters shown in Table 2. In this case,

$$\beta \times (k_1 + k_2)/(S_I \times k_{I-}) \gg 1, \quad \beta \times (k_1 + k_2)/(S_D \times k_{D-}) \gg 1, \quad \text{and} \quad \beta \times (k_1 + k_2) \gg \alpha \times k_H, \tag{B14}$$

and one obtains from Eqs. A69–A75, A60–A65, and A45–A46

$$U_A = 1 \tag{B15}$$

$$U_D = \psi \times (S_I \times k_{I-})/(S_D \times k_{D-}) + (1 - \psi) \tag{B16}$$

$$U_I = \psi + (1 - \psi) \times (S_D \times k_{D-})/(S_I \times k_{I-}) = U_D \times (S_D \times k_{D-})/(S_I \times k_{I-}) \tag{B17}$$

$$U_T = f_{T\alpha}/\{1 + [\alpha \times k_H/(S_I \times k_{I-})]/U_I\}, \tag{B18}$$

where $\psi = k_1/(k_1 + k_2)$ and $f_{T\alpha} = 1 + \alpha \times k_H/(S_T \times k_{T-})$ as defined by Eqs. A45 and A60.

At low phosphate concentrations $\psi \ll 1$, and Eqs. B15–B18 become

$$U_A = 1 \tag{B19}$$

$$U_D = 1 \tag{B20}$$

$$U_I = (S_D \times k_{D-})/(S_I \times k_{I-}) \tag{B21}$$

$$U_T = \{1 + \alpha \times k_H/(S_T \times k_{T-})\}/[1 + \alpha \times k_H/(S_D \times k_{D-})]. \tag{B22}$$

And at high phosphate concentrations, $\psi \sim 1$, and one obtains

$$U_A = 1 \tag{B23}$$

$$U_D = (S_I \times k_{I-})/(S_D \times k_{D-}) \tag{B24}$$

$$U_I = 1 \tag{B25}$$

$$U_T = \{1 + \alpha \times k_H/(S_T \times k_{T-})\}/[1 + \alpha \times k_H/(S_I \times k_{I-})]. \tag{B26}$$

In the absence of profilin,

$$U_T = (1 + \alpha \times k_H/k_{T-})/(1 + \alpha \times k_H/k_{Y-}), \tag{B27}$$

where index Y stands for either I or D. $Y = D$ is applicable for low (100 μM or less) and $Y = I$ for high (50–100 mM) Pi concentrations.

Note that variable α in Eqs. B12, B18, B22, B26, and B27 has an important meaning. It is related to the average length of the filament's ATP cap, L_{Cap}, which in turn is equal to the sum of probabilities $g_{T(i)}$ and $g_{PT(1)}$ for all subunits in the filament to carry ATP. The value $k_{HYD} = \alpha \times k_H \times g_{T(1)}$ is the total rate of hydrolysis per filament, and $\alpha \times g_{T(1)}$ is the length of the ATP cap in the absence of profilin or in the case when profilin does not accelerate ATP hydrolysis and $r_H = 1$. Indeed,

$$k_{HYD} = \sum k_H \times g_{T(i)} + k'_H \times g_{T(1)} \times P/K_{dbT}$$
$$= k_H \times (\sum g_{T(i)} - g_{T(1)} + g_{T(1)} \times S_H)$$
$$= k_H \times g_{T(1)} \times (g_f^{-1} \times \sum \lambda^i + S_H)$$
$$= g_{T(1)} \times k_H \times [S_H + g_f^{-1} \times \lambda/(1-\lambda)]$$
$$= \alpha \times k_H \times g_{T(1)} \quad \text{(B28)}$$

$$L_{Cap} = \sum g_{T(i)} + g_{T(1)} \times P/K_{dbT} = \sum g_{T(i)} - g_{T(1)}$$
$$+ g_{T(1)} \times q_T = g_{T(1)} \times (\alpha - S_H + q_T). \quad \text{(B29)}$$

Note that $S_H = q_T$ when $r_H = 1$ or $P = 0$. Then $k_{HYD} = L_{Cap} \times k_H$.

Stukalin and Kolomeisky (40), assuming vectorial hydrolysis, obtained a result similar to Eq. B27 for a one-step hydrolysis model which corresponds to our case (i) in the absence of profilin. Parameter $\alpha = 1$ for vectorial hydrolysis since at any moment only one ATP-bound end subunit in the filament can undergo hydrolysis (40,66) (in this case it is not associated with the length of the ATP cap).

Part 3: a hypothetical case when there is no (or very slow) ATP hydrolysis by F- or G-actin and no (or very slow) phosphate binding and release by F-actin

Note that in this case monomeric nucleotide exchange and phosphate binding and release must be at equilibrium (no mechanism II). That means that concentrations of monomeric actin nucleotide forms are defined simply by the affinities of the nucleotide-free actin to ATP and ADP and by the affinity of phosphate to monomeric ADP-actin according to Eqs. A82–A85. In the limit when the rates of hydrolysis and phosphate binding and release approach 0, coefficients U_n approach 1, and Eq. A68 reduces to

$$A_c \times \sum r_n \times A_{cn}^{-1} = 1. \quad \text{(B30)}$$

Then

$$A_c^{-1} = A_{ch0}^{-1} \equiv \sum r_n \times A_{cn}^{-1}. \quad \text{(B31)}$$

Indeed, since typically $K_{dn} < (k'_{n+}/k_{n+}) \times K_{dbn}$ (see Table 2), $S_n > q_n$ and

$$\sum (g_{n(1)} \times S_n) > \sum (g_{n(1)} \times q_n) = 1, \quad \text{(B32)}$$

then

$$E = \sum (g_{n(1)} \times S_n \times k_{n-}) \geq \min(k_{n-})$$
$$\times \sum (g_{n(1)} \times S_n) > \min(k_{n-}), \quad \text{(B33)}$$

$$k_H/E \ll 1, \quad \text{and} \quad (k_1 + k_2)/E \ll 1, \quad \text{when}$$
$$k_H/\min(k_{n-}) \ll 1, \quad \text{and} \quad (k_1 + k_2)/\min(k_{n-}) \ll 1. \quad \text{(B34)}$$

Under these conditions,

$$\alpha \approx g_f^{-1} \times [(E/k_H)^{1/2} + g_f \times S_H - 1] \quad \text{and}$$
$$\beta \approx g_f^{-1} \times [(E/(k_1 + k_2))^{1/2} + g_f \times S_{Pi} - 1]. \quad \text{(B35)}$$

Then if the values of r_H, r_{He}, r_{Pi}, r_{Pie}, K_{dn}, K_{dbn}, and k_{n-} are set constant and

$$k_H \to 0, \quad \text{and} \quad (k_1 + k_2) \to 0, \quad \text{(B36)}$$

one obtains

$$\alpha \times k_H/(S_n \times k_{n-}) \to 0; \quad \beta \times k_1/(S_n \times k_{n-}) \to 0;$$
$$\beta \times k_2/(S_n \times k_{n-}) \to 0; \quad \text{and} \quad U_n \to 1. \quad \text{(B37)}$$

In the absence of ATP hydrolysis and phosphate binding and release

$$U_n = 1; \lambda = \delta = 1. \quad \text{(B38)}$$

In this case the critical concentration A_{ch0} defined by Eq. B31 is a relatively simple combination of equilibrium constants and concentrations of nucleotides and organic phosphate. Note that in the absence of ATP hydrolysis, the binding of actin monomeric forms to profilin cannot change their distribution r_n due to the detailed balance constraints for monomeric reactions. Whether or not profilin is present, $A_c = A_{ch0}$ remains constant and does not depend on profilin concentration. This means that mechanism III is not possible at steady state.

Note also that from Eqs. A73–A81 and B37 follows that in the absence of ATP hydrolysis and inorganic phosphate release and binding to filamentous actin

$$g_n = r_n \times A_c \times A_{cn}^{-1} \quad \text{(B39)}$$

and Eq. A68 becomes

$$A_c \times \sum r_n \times A_{cn}^{-1} = \sum g_n = 1. \quad \text{(B40)}$$

APPENDIX 3: APPARENT ENERGY SQUARE AND PARAMETER Φ

As illustrated by Fig. 1, in the presence of profilin, there are two possible pathways for actin filament elongation: the direct pathway (pathway *g* shown with *gray arrow*), and the profilin-related pathway (pathway *pg* shown with *three purple arrows*). In the absence of profilin, there is only one pathway g_0. We designate the pathway *g* in the absence of profilin as a separate pathway g_0 because of prior experimental evaluations for the parameter Φ as explained below. According to Pantaloni and Carlier (7), the misbalance of the apparent energy square can be defined as

$$\Phi = [(k_-/k_+) \times K_{db}]/[(k'_-/k'_+) \times K_d]. \quad \text{(C1)}$$

The apparent parameters k_+, k'_+, k_-, k'_-, K_d, and K_{db} may be defined with the following equations:

$$k_{ON}^g = g_f \times k_+ \times [G] \quad \text{(C2)}$$
$$k_{ON}^{pg} = g_f \times k'_+ \times [PG] \quad \text{(C3)}$$
$$k_{OFF}^g = g_f \times k_- \quad \text{(C4)}$$
$$k_{OFF}^{pg} = (1 - g_f) \times k'_- \quad \text{(C5)}$$
$$K_d = P \times [G]/[PG] \quad \text{(C6)}$$
$$K_{db} = P \times g_f/(1 - g_f), \quad \text{(C7)}$$

where k_{ON}^g, k_{ON}^{pg}, k_{OFF}^g, and k_{OFF}^{pg} are the polymerization and depolymerization terms for pure G-actin and profilin-actin complex, correspondingly, and (see Eqs. A5–A7 and Eq. A21)

$$[G] = \sum n = A_c \quad \text{(C8)}$$
$$[PG] = \sum [Pn] \quad \text{(C9)}$$
$$k_{ON} = k_{ON}^g + k_{ON}^{pg} \quad \text{(C10)}$$
$$k_{OFF} = k_{OFF}^g + k_{OFF}^{pg} \quad \text{(C11)}$$
$$k_{ON}^g = g_f \times \sum (k_{n+} \times n) = g_f \times A_c \times \sum r_n \times k_{n+} \quad \text{(C12)}$$
$$k_{ON}^{pg} = g_f \times \sum (k'_{n+} \times [Pn])$$
$$= g_f \times A_c \times \sum r_n \times (S_n - 1) \times k_{n+} \quad \text{(C13)}$$

$$k^{g}_{OFF} = \sum g_{n(1)} \times k_{n-} \quad \text{(C14)}$$

$$k^{pg}_{OFF} = \sum (g_{Pn(1)} \times k'_{n-}) = \sum g_{n(1)} \times (S_n - 1) \times k_{n-}. \quad \text{(C15)}$$

Then one obtains from Eqs. C1–C15

$$\Phi = (k^{pg}_{ON}/k^{g}_{ON})/(k^{pg}_{OFF}/k^{g}_{OFF}), \quad \text{(C16)}$$

and

$$k_{+} = \sum r_n \times k_{n+} \quad \text{(C17)}$$

$$k'_{+} = ([G]/[PG]) \times \sum r_n \times (S_n - 1) \times k_{n+} \quad \text{(C18)}$$

$$k_{-} = g_f^{-1} \times \sum (g_{n(1)} \times k_{n-}) \quad \text{(C19)}$$

$$k'_{-} = (1 - g_f)^{-1} \times \sum g_{n(1)} \times (S_n - 1) \times k_{n-}. \quad \text{(C20)}$$

In the absence of profilin,

$$k_{0+} = \sum r_n \times k_{n+} \quad \text{(C21)}$$

$$k_{0-} = \sum g_{n(1)} \times k_{n-}. \quad \text{(C22)}$$

At conditions when the nucleotide exchange is fast $k_{0+} = k_{+}$ (compare Eqs. C17 and C21) although $k_{0-} \neq k_{-}$ since the values of $g_{n(1)}$ depend on profilin concentration. Therefore the pathway g for direct filament elongation in the presence of profilin is not energetically equivalent to the pathway g_0 for the direct filament elongation in the absence of profilin. Then, as discussed in the text, at least two different definitions for the parameter Φ are possible: $\Phi = \Phi_{pg-g}$ related to the energy difference between the polymerization pathways pg and g and parameter Φ_{pg-g0} related to the energy difference between polymerization pathways pg and g_0. It is also possible to compare the pathways g and g_0. Since dependence of the standard free energy change for the pathway g on profilin concentration had not been recognized by earlier investigators, prior experimental evaluations for the parameter Φ actually evaluate the difference between the pathways g_0 and pg, and therefore refer to Φ_{pg-g0} as Φ (2,7,14):

$$\Phi_{pg-g0} = [(k_{0-}/k_{0+}) \times K_{db}]/[(k'_{-}/k'_{+}) \times K_d] \quad \text{(C23)}$$

$$\Phi_{pg-g} = [(k_{-}/k_{+}) \times K_{db}]/[(k'_{-}/k'_{+}) \times K_d]. \quad \text{(C24)}$$

The value of Φ_{pg-g0} is related to the value of Φ_{pg-g} as

$$\Phi_{pg-g0} = \Phi_{pg-g} \times [(k_{0-}/k_{0+})]/[(k_{-}/k_{+})] = \Phi_{pg-g} \times (k_{0-}/k_{-}) \quad \text{(C25)}$$

since $k_{0+} = k_{+}$, and

$$\Phi_{pg-g} = (k^{pg}_{ON}/k^{g}_{ON})/(k^{pg}_{OFF}/k^{g}_{OFF}). \quad \text{(C26)}$$

(see Eq. C16). Note that

$$k_{0-}/k_{0+} = A_{c0}, \quad \text{and} \quad k_{-}/k_{+} \neq A_c = k_{OFF}/k_{ON}. \quad \text{(C27)}$$

Thus there are three pathways that may be compared for the energy difference: pg, g, and g_0, each with the corresponding standard free energy change: $\Delta G'^{0}_{pg}$, $\Delta G'^{0}_{g}$, $\Delta G'^{0}_{g0}$

$$\Delta G'^{0}_{pg} - \Delta G'^{0}_{g} = -RT \ \ln(\Phi_{pg-g}) \quad \text{(C28)}$$

$$\Delta G'^{0}_{pg} - \Delta G'^{0}_{g0} = -RT \ \ln(\Phi_{pg-g0}) \quad \text{(C29)}$$

$$\Delta G'^{0}_{g} - \Delta G'^{0}_{g0} = -RT \ \ln[(k_{0-}/k_{0+})]/[(k_{-}/k_{+})] = -RT \ \ln(k_{0-}/k_{-}). \quad \text{(C30)}$$

In addition, the difference in the standard free energy change for the combined polymerization through both pathways pg and g and the pathway g_0 is

$$\Delta G'^{0}_{(pg+g)} - \Delta G'^{0}_{g0} = -RT \ln(A_{c0}/A_c). \quad \text{(C31)}$$

Note that in the absence of mechanism IVb, i.e., when the values of r_{n+}/K_{dn} are equal for all forms, for all forms $S_n = S$ and

$$\Phi_{pg-g} = [(S-1) \times k^{g}_{ON}/k^{g}_{ON}]/[(S-1) \times k^{g}_{OFF}/k^{g}_{OFF}] = 1 \quad \text{(C32)}$$

for all profilin concentrations. This means that in the absence of mechanism IVb the pathways pg and g are energetically equivalent.

Note also that the standard free energy change for actin barbed-end polymerization in the absence of profilin and the presence of ATP hydrolysis $\Delta G'^{0}_{g0} = RT \ln(A_{c0})$ is larger than the standard free energy change for a hypothetical reaction for barbed-end polymerization in the presence of ATP and the absence of both profilin and ATP hydrolysis $\Delta G'^{0}_{g0h0} = RT \ln(A_{cT})$ (since both values are negative, the larger $\Delta G'^{0}_{g0}$ means a smaller absolute value). Profilin can partly eliminate the effect of hydrolysis, bringing $\Delta G'^{0}_{(pg+g)} < \Delta G'^{0}_{g0}$ (mechanism V) or even can convert hydrolysis from a factor working against polymerization to a factor that promotes polymerization, bringing $\Delta G'^{0}_{(pg+g)} < \Delta G'^{0}_{g0h0}$ (mechanism IVb). Note that in the absence of ATP hydrolysis, the standard free energy change should be the same in the presence and absence of profilin: $\Delta G'^{0}_{(pg+g)h0} = \Delta G'^{0}_{g0h0}$ and $\Delta G'^{0}_{(pg+g)h0} - \Delta G'^{0}_{g0} = -RT \ln(A_{c0}/A_{cT})$. The value of $\Delta G'^{0}_{(pg+g)h0} - \Delta G'^{0}_{g0}$ is shown in Fig. 8 *D* (*dashed gray line*).

We thank Ikuko Fujiwara for discussions and advice. The profilin-actin model is accessible to all readers through an interactive web page (31).

This work was supported by the Medical Research Service of the Department of Veterans Affairs, the National Institute of Arthritis and Musculoskeletal and Skin Diseases (NIAMS), grant No. 5K25AR048918 (to E.G.Y.), and the National Science Foundation, grant No. NSF-0316015 (to M.R.B.).

REFERENCES

1. Carlsson, L., L. E. Nystrom, U. Lindberg, K. K. Kannan, H. Cid-Dresdner, and S. Lovgren. 1976. Crystallization of a non-muscle actin. *J. Mol. Biol.* 105:353–366.
2. Kinosian, H. J., L. A. Selden, L. C. Gershman, and J. E. Estes. 2002. Actin filament barbed end elongation with nonmuscle MgATP-actin and MgADP-actin in the presence of profilin. *Biochemistry*. 41:6734–6743.
3. Bubb, M. R., E. G. Yarmola, B. G. Gibson, and F. S. Southwick. 2003. Depolymerization of actin filaments by profilin. Effects of profilin on capping protein function. *J. Biol. Chem.* 278:24629–24635.
4. Yarmola, E. G., and M. R. Bubb. 2004. Effects of profilin and thymosin β_4 on the critical concentration of actin demonstrated in vitro and in cell extracts with a novel direct assay. *J. Biol. Chem.* 279: 33519–33527.
5. Yarmola, E. G., and M. R. Bubb. 2006. Profilin: emerging concepts and lingering misconceptions. *Trends Biochem. Sci.* 31:197–205.
6. Tilney, L. G., E. M. Bonder, L. M. Coluccio, and M. S. Mooseker. 1983. Actin from Thyone sperm assembles on only one end of an actin filament: a behavior regulated by profilin. *J. Cell Biol.* 97:112–124.
7. Pantaloni, D., and M. F. Carlier. 1993. How profilin promotes actin filament assembly in the presence of thymosin β 4. *Cell*. 75:1007–1014.
8. Pollard, T. D., and J. A. Cooper. 1984. Quantitative analysis of the effect of Acanthamoeba profilin on actin filament nucleation and elongation. *Biochemistry*. 23:6631–6641.
9. Pring, M., A. Weber, and M. R. Bubb. 1992. Profilin-actin complexes directly elongate actin filaments at the barbed end. *Biochemistry*. 31: 1827–1836.

10. Weber, A. 1999. Actin binding proteins that change extent and rate of actin monomer-polymer distribution by different mechanisms. *Mol. Cell. Biochem.* 190:67–74.

11. Mockrin, S. C., and E. D. Korn. 1980. Acanthamoeba profilin interacts with G-actin to increase the rate of exchange of actin-bound adenosine 5′-triphosphate. *Biochemistry.* 19:5359–5362.

12. Kovar, D. R. 2005. Molecular details of formin-mediated actin assembly. *Curr. Opin. Cell Biol.* 18:11–17.

13. Romero, S., D. Didry, E. Larquet, N. Boisset, D. Pantaloni, and M. F. Carlier. 2007. How ATP hydrolysis controls filament assembly from profilin-actin: implication for formin processivity. *J. Biol. Chem.* 282: 8435–8445.

14. Kang, F., D. L. Purich, and F. S. Southwick. 1999. Profilin promotes barbed-end actin filament assembly without lowering the critical concentration. *J. Biol. Chem.* 274:36963–36972.

15. Perelroizen, I., D. Didry, H. Christensen, N. H. Chua, and M. F. Carlier. 1996. Role of nucleotide exchange and hydrolysis in the function of profilin in action assembly. *J. Biol. Chem.* 271:12302–12309.

16. Selden, L. A., H. J. Kinosian, J. E. Estes, and L. C. Gershman. 1999. Impact of profilin on actin-bound nucleotide exchange and actin polymerization dynamics. *Biochemistry.* 38:2769–2778.

17. Gutsche-Perelroizen, I., J. Lepault, A. Ott, and M. F. Carlier. 1999. Filament assembly from profilin-actin. *J. Biol. Chem.* 274:6234–6243.

18. Carlier, M. F., and D. Pantaloni. 1986. Direct evidence for ADP-Pi-F-actin as the major intermediate in ATP-actin polymerization. Rate of dissociation of Pi from actin filaments. *Biochemistry.* 25: 7789–7792.

19. Romero, S., C. Le Clainche, D. Didry, C. Egile, D. Pantaloni, and M. F. Carlier. 2004. Formin is a processive motor that requires profilin to accelerate actin assembly and associated ATP hydrolysis. *Cell.* 119: 419–429.

20. Dickinson, R. B., L. Caro, and D. L. Purich. 2004. Force generation by cytoskeletal filament end-tracking proteins. *Biophys. J.* 87:2838–2854.

21. Dickinson, R. B., F. S. Southwick, and D. L. Purich. 2002. A direct-transfer polymerization model explains how the multiple profilin-binding sites in the actoclampin motor promote rapid actin-based motility. *Arch. Biochem. Biophys.* 406:296–301.

22. Wegner, A. 1976. Head to tail polymerization of actin. *J. Mol. Biol.* 108:139–150.

23. Brenner, S. L., and E. D. Korn. 1983. On the mechanism of actin monomer-polymer subunit exchange at steady state. *J. Biol. Chem.* 258: 5013–5020.

24. Bindschadler, M., E. A. Osborn, C. F. Dewey Jr., and J. L. McGrath. 2004. A mechanistic model of the actin cycle. *Biophys. J.* 86:2720–2739.

25. Kouyama, T., and K. Mihashi. 1981. Fluorimetry study of *N*-(1-pyrenyl)iodoacetamide-labelled F-actin. Local structural change of actin protomer both on polymerization and on binding of heavy meromyosin. *Eur. J. Biochem.* 114:33–38.

26. Yarmola, E. G., S. Parikh, and M. R. Bubb. 2001. Formation and implications of a ternary complex of profilin, thymosin β_4, and actin. *J. Biol. Chem.* 276:45555–45563.

27. Yarmola, E. G., T. Somasundaram, T. A. Boring, I. Spector, and M. R. Bubb. 2000. Actin-latrunculin a structure and function: differential modulation of actin-binding protein function by latrunculin A. *J. Biol. Chem.* 275:28120–28127.

28. Vinson, V. K., E. M. De La Cruz, H. N. Higgs, and T. D. Pollard. 1998. Interactions of Acanthamoeba profilin with actin and nucleotides bound to actin. *Biochemistry.* 37:10871–10880.

29. Sept, D., J. Xu, T. D. Pollard, and J. A. McCammon. 1999. Annealing accounts for the length of actin filaments formed by spontaneous polymerization. *Biophys. J.* 77:2911–2919.

30. Kovar, D. R., J. R. Kuhn, A. L. Tichy, and T. D. Pollard. 2003. The fission yeast cytokinesis formin Cdc12p is a barbed end actin filament capping protein gated by profilin. *J. Cell Biol.* 161:875–887.

31. ABAKUS. http://ABAKUS.medicine.ufl.edu/.

32. Kuhn, J. R., and T. D. Pollard. 2005. Real-time measurements of actin filament polymerization by total internal reflection fluorescence microscopy. *Biophys. J.* 88:1387–1402.

33. Pollard, T. D. 1986. Rate constants for the reactions of ATP- and ADP-actin with the ends of actin filaments. *J. Cell Biol.* 103:2747–2754.

34. Oosawa, F., and S. Asakura. 1975. Thermodynamics of the Polymerization of Proteins. Academic Press, New York.

35. Fujiwara, I., D. Vavylonis, and T. D. Pollard. 2007. Polymerization kinetics of ADP- and ADP-Pi-actin determined by fluorescence microscopy. *Proc. Natl. Acad. Sci. USA.* 104:8827–8832.

36. Rickard, J., and P. Sheterline. 1986. Cytoplasmic concentrations of inorganic phosphate affect the critical concentration for assembly of actin in the presence of cytochalasin D or ADP. *J. Mol. Biol.* 191:273–280.

37. Weber, A., C. R. Pennise, and V. M. Fowler. 1999. Tropomodulin increases the critical concentration of barbed end-capped actin filaments by converting ADP·P_i-actin to ADP-actin at all pointed filament ends. *J. Biol. Chem.* 274:34637–34645.

38. Carlier, M. F., and D. Pantaloni. 1988. Binding of phosphate to F-ADP-actin and role of F-ADP-Pi-actin in ATP-actin polymerization. *J. Biol. Chem.* 263:817–825.

39. Kinosian, H. J., L. A. Selden, C. Lewis, L. C. Gershman, and J. E. Estes. 2000. Interdependence of profilin, cation, and nucleotide binding to vertebrate non-muscle actin. *Biochemistry.* 39:13176–13188.

40. Stukalin, E. B., and A. B. Kolomeisky. 2006. ATP hydrolysis stimulates large length fluctuations in single actin filaments. *Biophys. J.* 90:2673–2685.

41. Blanchoin, L., and T. D. Pollard. 2002. Hydrolysis of ATP by polymerized actin depends on the bound divalent cation but not profilin. *Biochemistry.* 41:597–602.

42. Kovar, D. R., E. S. Harris, R. Mahaffy, H. N. Higgs, and T. D. Pollard. 2006. Control of the assembly of ATP- and ADP-actin by formins and profilin. *Cell.* 124:423–435.

43. Perelroizen, I., M. F. Carlier, and D. Pantaloni. 1995. Binding of divalent cation and nucleotide to G-actin in the presence of profilin. *J. Biol. Chem.* 270:1501–1508.

44. Sablin, E. P., J. F. Dawson, M. S. VanLoock, J. A. Spudich, E. H. Egelman, and R. J. Fletterick. 2002. How does ATP hydrolysis control actin's associations? *Proc. Natl. Acad. Sci. USA.* 99:10945–10947.

45. Vologodskii, A. 2006. Energy transformation in biological molecular motors. *Phys. Life Rev.* 3:119–132.

46. Astumian, R. D. 1997. Thermodynamics and kinetics of a Brownian motor. *Science.* 276:917–922.

47. Ait-Haddou, R., and W. Herzog. 2003. Brownian ratchet models of molecular motors. *Cell Biochem. Biophys.* 38:191–214.

48. Tomkiewicz, D., N. Nouwen, and A. J. Driessen. 2007. Pushing, pulling and trapping–modes of motor protein supported protein translocation. *FEBS Lett.* 581:2820–2828.

49. Simon, S. M., C. S. Peskin, and G. F. Oster. 1992. What drives the translocation of proteins? *Proc. Natl. Acad. Sci. USA.* 89:3770–3774.

50. Konevega, A. L., N. Fischer, Y. P. Semenkov, H. Stark, W. Wintermeyer, and M. V. Rodnina. 2007. Spontaneous reverse movement of mRNA-bound tRNA through the ribosome. *Nat. Struct. Mol. Biol.* 14:318–324.

51. Lizunov, V., and J. Zimmerberg. 2006. Cellular biophysics: bacterial endospore, membranes and random fluctuation. *Curr. Biol.* 16:R1025–R1028.

52. Broder, D. H., and K. Pogliano. 2006. Forespore engulfment mediated by a ratchet-like mechanism. *Cell.* 126:917–928.

53. Saffarian, S., H. Qian, I. Collier, E. Elson, and G. Goldberg. 2006. Powering a burnt bridges Brownian ratchet: a model for an extracellular motor driven by proteolysis of collagen. *Phys. Rev. E Stat. Nonlin. Soft Matter Phys.* 73:041909.

54. Hinrichsen, L., A. Meyerholz, S. Groos, and E. J. Ungewickell. 2006. Bending a membrane: how clathrin affects budding. *Proc. Natl. Acad. Sci. USA.* 103:8715–8720.

55. Raj, A., and C. S. Peskin. 2006. The influence of chromosome flexibility on chromosome transport during anaphase A. *Proc. Natl. Acad. Sci. USA.* 103:5349–5354.

56. Abbondanzieri, E. A., W. J. Greenleaf, J. W. Shaevitz, R. Landick, and S. M. Block. 2005. Direct observation of base-pair stepping by RNA polymerase. *Nature*. 438:460–465.

57. Park, S., D. Koch, R. Cardenas, J. Kas, and C. K. Shih. 2005. Cell motility and local viscoelasticity of fibroblasts. *Biophys. J*. 89:4330–4342.

58. Qian, H. 2004. A stochastic analysis of a Brownian ratchet model for actin-based motility. *Mech. Chem. Biosyst.* 1:267–278.

59. Burroughs, N. J., and D. Marenduzzo. 2005. Three-dimensional dynamic Monte Carlo simulations of elastic actin-like ratchets. *J. Chem. Phys.* 123:174908.

60. van Oudenaarden, A., and J. A. Theriot. 1999. Cooperative symmetry-breaking by actin polymerization in a model for cell motility. *Nat. Cell Biol.* 1:493–499.

61. Mogilner, A., and G. Oster. 1996. Cell motility driven by actin polymerization. *Biophys. J*. 71:3030–3045.

62. Astumian, R. D. 2000. The role of thermal activation in motion and force generation by molecular motors. *Philos. Trans. R. Soc. Lond. B Biol. Sci.* 355:511–522.

63. Astumian, R. D., and I. Derenyi. 1998. Fluctuation driven transport and models of molecular motors and pumps. *Eur. Biophys. J*. 27:474–489.

64. Astumian, R. D. 2002. Protein conformational fluctuations and free-energy transduction. *Appl. Phys. A*. 75:193–206.

65. Wang, H., and G. Oster. 1998. Energy transduction in the F_1 motor of ATP synthase. *Nature*. 396:279–282.

66. Carlier, M. F., D. Pantaloni, and E. D. Korn. 1987. The mechanisms of ATP hydrolysis accompanying the polymerization of Mg-actin and Ca-actin. *J. Biol. Chem.* 262:3052–3059.